

Probe Report

Title: Identification of Inhibitors of *Trypanosoma brucei* Hexokinases

Authors: Elizabeth Sharlow^{1,2}, Jennifer E. Golden³, Heidi Dodson⁴, Meredith Morris⁴, Marcia Hesser⁴, Todd Lyda⁴, Stephanie Leimgruber^{1,2}, Chad E. Schroeder³, Dan P. Flaherty³, Warren S. Weiner³, Denise Simpson³, John S. Lazo^{1,2}, Jeffrey Aubé^{3,5,6}, and James C. Morris⁴

¹University of Pittsburgh Drug Discovery Institute and Pittsburgh Molecular Libraries Screening Center, University of Pittsburgh, Pittsburgh, PA

²Department of Pharmacology and Chemical Biology, University of Pittsburgh, Pittsburgh, PA

³University of Kansas Specialized Chemistry Center

⁴Department of Genetics and Biochemistry, Clemson University, Clemson, SC

⁵Department of Medicinal Chemistry, University of Kansas, Lawrence, KS

⁶Corresponding author's email: jaube@ku.edu

Assigned Assay Grant #: 1 R03 MH082340-01A1

Screening Center & PI: Pittsburgh Screening Center (MLSCN), John Lazo

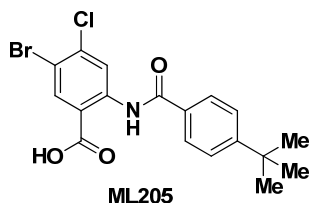
Chemistry Center & PI: University of Kansas Specialized Chemistry Center, Jeffrey Aubé

Assay Submitter & Institution: James C. Morris, Clemson University

PubChem Summary Bioassay Identifier (AID): AID 2600

Abstract: The unicellular eukaryote *Trypanosoma brucei* (*T. brucei*) is the causative agent of human African trypanosomiasis (HAT), a disease that annually infects ~500,000 people in sub-Saharan Africa resulting in 50,000 – 70,000 deaths per year. Without treatment, HAT is fatal. Unfortunately, current treatments are limited in availability, have toxic side effects, are difficult to administer and are not well characterized in terms of their mechanism of action. Thus, the lack of affordable, safe, and effective therapies for those with African trypanosomiasis makes the identification of molecular target-specific chemotypes a priority in our effort to understand the mechanisms involved with parasite growth and viability, as well as for future therapeutic development. The probe identified from this effort, ML205, is a stable, small molecule possessing submicromolar activity ($IC_{50} = 0.98 \mu\text{M}$) against a defined *T. brucei* hexokinase 1 (rTbHK1) target. The probe was not toxic to mammalian cells (IMR-90 cells, $EC_{50} > 25 \mu\text{M}$) and mechanistic studies revealed that the probe operates with mixed inhibition with respect to ATP.

Probe Structure & Characteristics:



CID/ML#	Target Name	IC ₅₀ /EC ₅₀ (nM) [SID, AID]	Anti-target Name(s)	IC ₅₀ /EC ₅₀ (μM) [SID, AID]	Fold Selective	Secondary Assay(s) Name: IC ₅₀ /EC ₅₀ (nM) [SID, AID]
CID 46931017 ML205	TbHK1	IC ₅₀ = 976 nM (SID 99437306, AID 2230)	G6PDH and hGik	G6PDH IC ₅₀ > 25000 nM; (SID 99437306, AID 2579) hGik IC ₅₀ = 48300 nM; (SID 99437306, AID 492951)	G6PDH:TbHK1 = 25.5 hGik:TbHK1 = 49.3	IMR-90 cell viability assay; EC ₅₀ > 25000 nM; (SID 99437306, AID 449725)

Recommendations for scientific use of the probe:

What limitations in current state of the art is the probe addressing: The unicellular eukaryote *Trypanosoma brucei* (*T. brucei*) is the causative agent of human African trypanosomiasis (HAT), a disease that annually infects ~500,000 people in sub-Saharan Africa resulting in 50,000 – 70,000 deaths per year. Disease manifestation consists of the haemolymphatic and neurological phases, the latter of which begins when the *T. brucei* parasites cross the blood brain barrier and invade the central nervous system. Without treatment, HAT is fatal. Unfortunately, current treatments are limited in availability, have toxic side effects, are difficult to administer and are not well characterized in terms of their mechanism of action. There are only four drugs approved for treatment of HAT. Suramin and pentamidine, however, are not effective against the neurological stage of HAT while melarsoprol leads to fatal complications in 5–10% of patients receiving the drug. The most recently developed drug, eflornithine, is expensive and only efficacious against *T. b. gambiense*, but is curative in both stages of the disease. However, delivery of eflornithine is difficult, as the compound must be administered intravenously four times a day for 14 days. Thus, the lack of affordable, safe, and effective therapies for those with African trypanosomiasis makes the identification of molecular target-specific chemotypes a priority in our effort to understand the mechanisms involved with parasite growth and viability, as well as for future therapeutic development [1, 2]. The probe identified from this effort, ML205, is a stable, small molecule possessing submicromolar activity against a defined *T. brucei* hexokinase 1 (TbHK1) target with mixed inhibition with respect to ATP.

What will the probe be used for: The assay provider is currently using the probe to investigate the nature of TbHK1 inhibition and is interested to use this as the starting point for further characterization, aimed ultimately at demonstrating *in vivo* efficacy and providing a lead for advanced development in the treatment of HAT. The probe was the subject of a probe

enhancement proposal, submitted to the NIH on October 13, 2010, and recently funded as a grant proposal. In this regard, the probe will be used as a means of demonstrating (a) TbHK1 on target activity via an orthogonal ATP-regeneration coupled assay, (b) impact on parasitic cell growth potential in a live/dead BSF assay, (c) efficacy against a related parasite using a whole parasite-based, *Leishmania* promastigote assay, (d) action on the *in vivo* target, (e) TbHK1 activity from *T. brucei* parasite lysate with IC_{50} similar to recombinant protein, (f) adequate *in vivo* PKDM properties leading to (g) showing efficacy in an acute infection mouse model. As outlined above, to truly impact this disease and the people affected by it, there is a dire need to identify better performing leads, further understand the mechanism by which compounds can inhibit *T. brucei* effectively, and ultimately halt the associated disease that is treated inadequately with currently available agents. This probe will establish a target-based approach of disease interference for HAT.

Who in the research community will use the probe: The assay provider will be using the probe for the purposes described above. The probe will be useful to groups interested in identifying resistance pathways in the parasite, particularly in collaboration with the powerful forward genetic tools available in the *T. brucei* system. Moreover, if the compound has efficacy in a mouse model, suggesting it is a lead compound that merits further development for this important neglected tropical-disease, interest will be wide-spread.

What is the relevant biology to which the probe can be applied: The development of lead compounds targeting various pharmacology for the treatment of human African trypanosomiasis was recently reviewed [3]. A TbHK1 small molecule probe is of particular interest because of the importance of glucose metabolism to the infectious bloodstream form (BSF) lifecycle stage of the parasite. Specifically, in the mammalian host, the *T. brucei* BSF parasite generates ATP exclusively through glycolysis. Hexokinase (HK), the first enzyme in glycolysis, catalyzes the transfer of the γ -phosphoryl group of ATP to glucose yielding glucose-6-phosphate. Several lines of evidence indicate that inhibition of TbHK1 activity in BSF parasites is lethal [4, 5]. Previously, the Assay Provider (Dr. James Morris, Clemson University) demonstrated that recombinant TbHK1 (rTbHK1) is inhibited by lonidamine ($IC_{50} = 850 \mu M$), an anti-cancer drug that targets tumor hexokinases, and the compound is toxic to *T. brucei* [6]. Furthermore, the HTS effort sponsored by this project has revealed potent anti-parasitics against the recombinant enzyme, suggesting that through careful SAR development, inhibitors of TbHK1 can be identified that will be useful lead compounds for the development of anti-trypanosomal agents.

1 Introduction

Probe Project Purpose: There is a significant need to identify new agents that effectively address human African trypanosomiasis (HAT), as current treatments are limited in number and availability, have toxic side effects, are difficult to administer or are not well characterized in terms of their mechanism of action. The purpose of this probe project was to identify a small molecule, single-digit micromolar range inhibitor of recombinant *T. brucei* hexokinase 1 (TbHK1) which would provide a good lead for further development and establish a target-based approach of potentially treating HAT.

Prior Art Status: There are only four drugs approved for treatment of HAT (Fig. 1). However, suramin and pentamidine are not effective against the neurological stage of HAT and melarsoprol leads to fatal complications in 5–10% of patients receiving the drug. The most recently developed drug, eflornithine, is expensive and only efficacious against *T. b. gambiense* (one of three known species), but is curative in both stages of the disease. However, delivery of eflornithine is difficult, as the compound must be administered intravenously four times a day for 14 days. Thus, the lack of affordable, safe, and effective therapies for those with African trypanosomiasis makes the identification of molecular target-specific chemotypes a priority in our effort to understand the mechanisms involved with parasite growth and viability, as well as for future therapeutic development [1, 2].

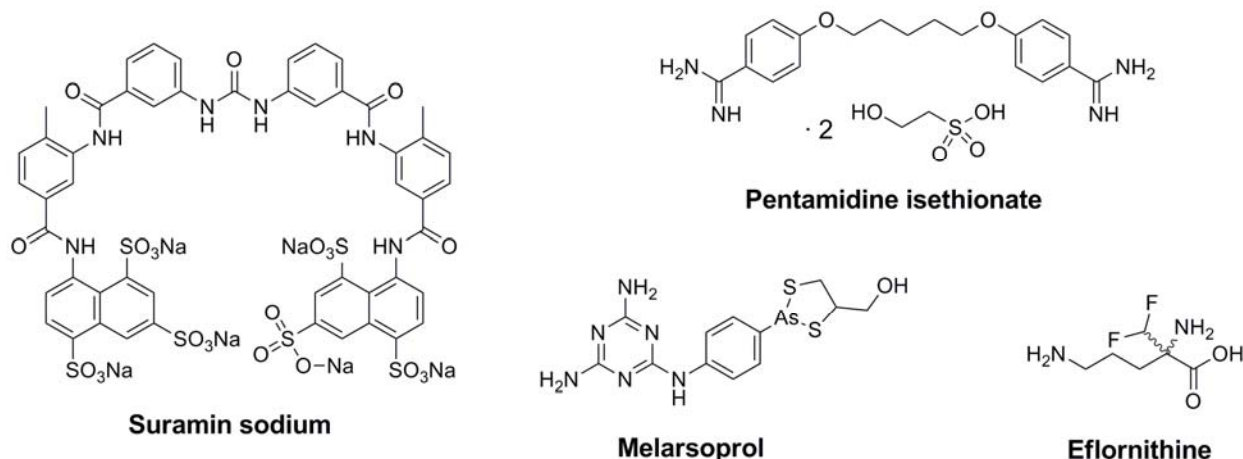
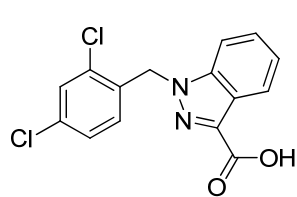
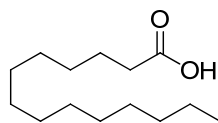
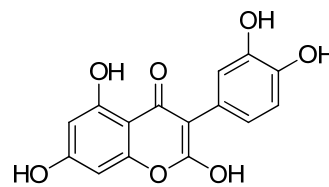


Figure 1. Currently available marketed drugs for treatment of human African trypanosomiasis

Recently, the Assay Provider (Dr. James Morris, Clemson University) demonstrated that recombinant TbHK1 (rTbHK1) is inhibited by lonidamine ($IC_{50} = 850 \mu\text{M}$), an anti-cancer drug that targets tumor hexokinases (Fig. 2) [6]. Lonidamine also inhibits HK activity from whole parasite lysate ($IC_{50} = 965 \mu\text{M}$) and is toxic to cultured bloodstream form parasites ($LD_{50} = 50 \mu\text{M}$). Myristic acid and quercetin were also reported to inhibit rTbHK1 at IC_{50} values of $78 \mu\text{M}$ and $85 \mu\text{M}$, respectively [7]. Thus, for the duration of this project, to our knowledge no potent and specific small molecule inhibitors of TbHK1 existed.


Ionidamine

 TbHK1 IC₅₀ = 850 μM

myristic acid

 TbHK1 IC₅₀ = 78 μM

quercetin

 TbHK1 IC₅₀ = 85 μM

Figure 2. Known TbHK1 inhibitors and preliminary associated data

The Assay Provider recently undertook an independent study of quercetin and determined the rTbHK1 IC₅₀ to be 4.1 ± 0.8 μM [8]. Given the discrepancy of rTbHK1 inhibition data associated with quercetin, the KU SCC obtained a commercial source of the material, purified it by reverse-phase chromatography, and performed a rigorous analytical analysis for structural integrity and purity assessment. This sample was then evaluated in the same rTbHK1 *in vitro* assay that was used for assessment of analogs for this project. Additionally, the Pittsburgh Screening Center supplied its own sample of quercetin in a side-by-side analysis. Depending on the source of the material, there was an observed variance in rTbHK1 inhibition (Table 1).

Table 1. Comparison of data obtained with variable quercetin sources

Entry	Source	Numerical identifier	Form of compound	Solids purified and QC analysis performed?	Source of assay data	TbHK1 IC ₅₀ μM
1	Spectrum Chemical Manufacturing Corp	order # Q2150, CAS# 6151-25-3	Quercetin, Dihydrate	No	Assay Provider's lab	4.1 ± 0.80
2	EMD Biosciences	order 551600, CAS# 6151-25-3	Quercetin, Dihydrate	No	Pittsburgh Screening Center	64.9 ± 18.5
3	KU SCC*	SID 99460891	Quercetin	Yes	Pittsburgh Screening Center	22.4 ± 0.30

*KU SCC obtained material from Sigma Aldrich, order number Q4951; CAS# 117-39-5

While the team has not definitely established the underlying cause for the observed range in activity, it has been reasoned that the well-established antioxidant nature of the flavinol structure renders this class of compounds susceptible to gradual transformation which could give rise to contaminants in the sample. A rigorous purification and analysis of material prior to assay revealed an rTbHK1 IC₅₀ = 22.4 μM. The team is interested in following up further on suspected contaminants in non-purified samples that might be contributing to the observed low micromolar inhibition of TbHK1. In any event, quercetin is the most relevant TbHK1 inhibitor due to its activity to which a new probe should be compared. Like Ionidamine, quercetin (unpurified) has

also been shown to inhibit hexokinase activity from whole parasite lysate ($IC_{50} = 24 \mu M$), and is toxic to cultured bloodstream form parasites ($LD_{50} = 7.5 \mu M$) [8]. Importantly, quercetin has been reported to engage other mammalian enzymes such as a tyrosine protein kinase, a phosphorylase kinase [9] a phosphatidyl 3-kinase [10] and a DNA topoisomerase [11]. The inhibition of these targets is in the IC_{50} range of 3-300 μM , which coincides with that for TbHK1, thereby suggesting that there may be only limited opportunities to increase the therapeutic range for the compound [8]. Moreover, a more selective probe with few off-target effects would greatly facilitate the study of how to effectively inhibit TbHK1 and provide a better lead positioned for development of HAT therapeutics.

2 Materials and Methods

2.1 Assays

A. Primary HTS TbHK1 Assay:

Descriptive Name: Inhibition of TbHK1 using glucose 6-phosphate dehydrogenase and monitoring depletion of NAD^+ at a single concentration (10 μM).

Purpose: The purpose of this assay is to identify compounds that act as TbHK1 small molecule inhibitors in HTS format at a single concentration of 10 μM .

Summary AID: AID 2600

Assigned AID: AID 1430

Screening Responsibility: Pittsburgh Molecular Libraries Screening Center (MLSCN), John S. Lazo

Non-phenotypic Assay; Non-multiplexed Assay; BSL: BSL1

Assay Format: biochemical

Assay Type: enzymatic

Assay Method: endpoint assay

Assay Detection: absorbance

Target type: kinase

Assay Description: The biochemical, absorbance-based assay used for HTS implementation employs recombinant TbHK1 protein and glucose and ATP as the substrates in a coupled reaction. In this assay, commercially available glucose 6-phosphate dehydrogenase is included as a coupling enzyme to reduce NAD^+ to NADH (which can be monitored spectrophotometrically at 340 nm) during the oxidation of glucose-6-P to 6-phosphogluconic acid. This assay was performed in a 384 well format and each assay plate contained 32 Maximum (vehicle; 1% DMSO), 24 Minimum (133 μM) and 8 IC_{50} control (1.3 μM) wells. These controls were used to derive the Z-factor and signal to background of each assay plate. Assay plates were passed and/failed according to the derived Z-factors. To account for possible inhibition of the other enzymes in the primary coupled reaction, putative inhibitors

were screened to assess their impact against glucose-6-phosphate dehydrogenase counter-screening assay [7].

B. Primary TbHK1 Assay for SAR:

Descriptive Name: Inhibition of TbHK1 using glucose 6-phosphate dehydrogenase and monitoring depletion of NAD⁺ - 10 point concentration response assay.

Purpose: This assay is the same as the HTS screen; however, the compounds are evaluated over 10-20 concentrations in a dose response format.

Summary AID: AID 2600

Assigned AID: AID 1632

Screening Responsibility: Pittsburgh Molecular Libraries Screening Center (MLSCN), John S. Lazo

Non-phenotypic Assay; Non-multiplexed Assay; BSL: BSL1

Assay Format: biochemical

Assay Type: enzymatic

Assay Method: endpoint assay

Assay Detection: absorbance

Target Type: kinase

Assay Description: The biochemical, absorbance-based assay used for HTS implementation employs recombinant TbHK1 protein and glucose and ATP as the substrates in a coupled reaction. In this assay, commercially available glucose 6-phosphate dehydrogenase is included as a coupling enzyme to reduce NAD⁺ to NADH (which can be monitored spectrophotometrically at 340 nm) during the oxidation of glucose-6-P to 6-phosphogluconic acid. This assay was performed in a 384 well format and each assay plate contained 32 Maximum (vehicle; 1% DMSO), 24 Minimum (133 μ M) and 8 IC₅₀ control (1.3 μ M) wells. These controls were used to derive the Z-factor and signal to background of each assay plate. Assay plates were passed and/failed according to the derived Z-factors. To account for possible inhibition of the other enzymes in the primary coupled reaction, putative inhibitors were screened to assess their impact against glucose-6-phosphate dehydrogenase counter-screening assay. Compounds are evaluated at 10-20 concentrations [7].

C. Secondary G6PDH Assay:

Descriptive Name: G6PDH Coupled Enzyme Counter Screen

Purpose: The purpose of this assay is to identify and remove false positives from consideration that interfere with the primary assay by interfering with the reporter enzyme, G6PDH.

Summary AID: AID 2600

Assigned AID: AID 2516

Screening Responsibility: Pittsburgh Molecular Libraries Screening Center (MLSCN), John S. Lazo

Non-phenotypic Assay; Non-multiplexed Assay; BSL: BSL1

Assay Format: biochemical

Assay Type: enzymatic

Assay Method: endpoint assay

Assay Detection: absorbance

Target type: cellular pathway

Assay Description: This assay is a modification of the primary assay, with glc6P supplemented in the reaction and ATP, glucose and TbHK1 removed in order to measure the activity of the reporter enzyme, G6PDH. For primary screening, compounds will be excluded if inhibit G6DPH >50% of signal readout. For IC₅₀ determinations, G6DPH inhibition would be 10x greater than inhibition of TbHK1 [7].

D. Secondary IMR-90 Assay

Descriptive Name: Human IMR90 Growth Inhibition Assay

Purpose: The purpose of this assay is to assess impact of compounds on human cell line while showing efficacious toxicity against *T. brucei*.

Summary AID: AID 2600

Assigned AID: AID 449725

Screening Responsibility: Pittsburgh Molecular Libraries Screening Center (MLSCN), John S. Lazo

Phenotypic Assay; Non-multiplexed Assay; BSL: BSL1

Assay Format: live, cell-based

Assay Type: viability/toxicity

Assay Method: endpoint assay

Assay Detection: fluorescence intensity

Target type: cellular pathway

Assay Description: This is a Alamar-blue based viability assay. IMR90 cells are cultured and maintained according to ATCC specifications (ATCC, Manassas, VA). IMR90 line drug susceptibility assays are performed in final volumes of 25 μ L using a 384-well assay format. Briefly, 1,000 cells/22 μ L in complete culture medium are seeded into each well of 384-well microtiter plates using a Titertek MAPC-2 bulk dispenser. Test and control compounds are added to individual wells (3 μ L/well). Vehicle and positive controls are 1% DMSO and 10% DMSO, respectively (final well concentrations). Assay plates are incubated for 44h at 37°C in the presence of 5% CO₂ and growth inhibitory effects are determined after the addition of 5 μ L/well of Alamar blue reagent (incubate 4 hr). Data are captured on a Molecular Devices SpectraMax M5 platereader [7].

E. Secondary BSF live/dead Assay - NOT REQUIRED FOR PROBE CRITERIA:

Descriptive Name: *T. brucei* parasite toxicity assay

Purpose: The purpose of this assay is to assess compounds in their ability to inhibit cell growth of *T. brucei* parasites.

Screening Responsibility: Assay provider, James Morris, Clemson University

Phenotypic Assay; Non-multiplexed Assay; BSL: BSL2

Assay Format: live, cell-based

Assay Type: viability/toxicity

Assay Method: endpoint assay

Assay Detection: fluorescence intensity

Target type: cellular pathway

Assay Description: This assay is an adaptation to a 96-well format of an Alamar blue-based cell viability assay (using Cell-Titer Blue) that measures the reduction of resazurin to resorufin by cellular processes. To determine the impact of TbHK1 inhibitors on cell growth, parasites are seeded at 5×10^3 BSF parasites (cell line 90-13, a 427 strain) into 96-well clear-bottomed polystyrene plates in 200 μ l HMI-9 supplemented with 10% fetal bovine serum and 10% Serum Plus (Sigma-Aldrich, St. Louis, MO) and grown in the presence of compound (2 μ l) or equivalently diluted carrier for 3 days in 5% CO₂ at 37°C. CellTiter Blue (Promega, Madison WI) is added (20 μ l) and the plates incubated an additional 3 hr under standard culture conditions. Fluorescence emission at 585 nm is then measured after excitation at 546 nm in a GENios microtiter plate reader (Phenix Research Products, Hayward CA) [7].

F. Secondary hGlc Assay

Descriptive Name: Human Glucokinase (hGlc) Counter Screen Assay

Purpose: The purpose of this assay is to identify compounds that are nonselective or possess potentially undesirable cross reactivity, due to inhibition of the related enzyme, hGlc.

Screening Responsibility: Assay provider, James Morris

Summary AID: AID 2600

Assigned AID: AID 492951

Non-phenotypic Assay; Non-multiplexed Assay; BSL: BSL1

Assay Format: biochemical

Assay Type: enzymatic

Assay Method: kinetic

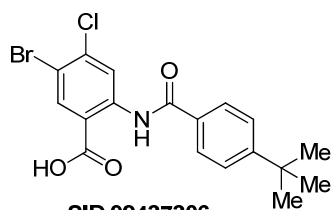
Assay Detection: absorbance

Target type: kinase

Assay Description: This assay uses human HK 4 (*i.e.*, human glucokinase, hGK, GenBank accession no. BC001890) expressed from a cloned cDNA (OPEN Biosystems, Huntsville, AL) in pQE30. After sequencing, the plasmid is transformed into *E. coli* M15 (pREP) and cultures are grown to an OD600 of 0.9 in terrific broth and protein expression induced (3 hr, 37°C) with 1 mM IPTG, followed by purification by nickel affinity chromatography. Ideally, IC₅₀s for hGK will be >10 μM. Please note that while we prefer selective inhibitors of TbHK1, inhibition of the human enzyme does not indicate removal from consideration, as the trypanosome is exclusively reliant on TbHK1 for metabolism, while host organisms (including humans) have a varied metabolism and redundancies that may allow them to tolerate inhibition of related enzymes [7].

2.2 Probe Chemical Characterization

A. Probe Chemical Structure, Physical Parameters and Probe Properties:



SID 99437306
 CID 46931017
 ML205

Molecular Formula: C₁₈H₁₇BrClNO₃ **Purity (LCMS, 215 nm):** 100%
Molecular Weight: 410.69 [g/mol] **Melting Point:** 273-276 °C
Exact Mass: 409.01 [g/mol] **Physical State:** white solid
CLogP: 6.74
Topological Polar Surface Area: 66
Solubility (PBS buffer, pH 7.4): 25.6 μg/mL
Stability (% remaining after 48 h): 100%

B. Structure Verification and Purity: ¹H NMR, ¹³C NMR, LCMS and HRMS

Proton and carbon NMR data for ML205 SID 99437306, CID 46931017: Detailed analytical methods and instrumentation are described in section 2.3, entitled "Probe Preparation" under general experimental and analytical details. The numerical experimental proton and carbon data are represented below, along with the associated spectra.

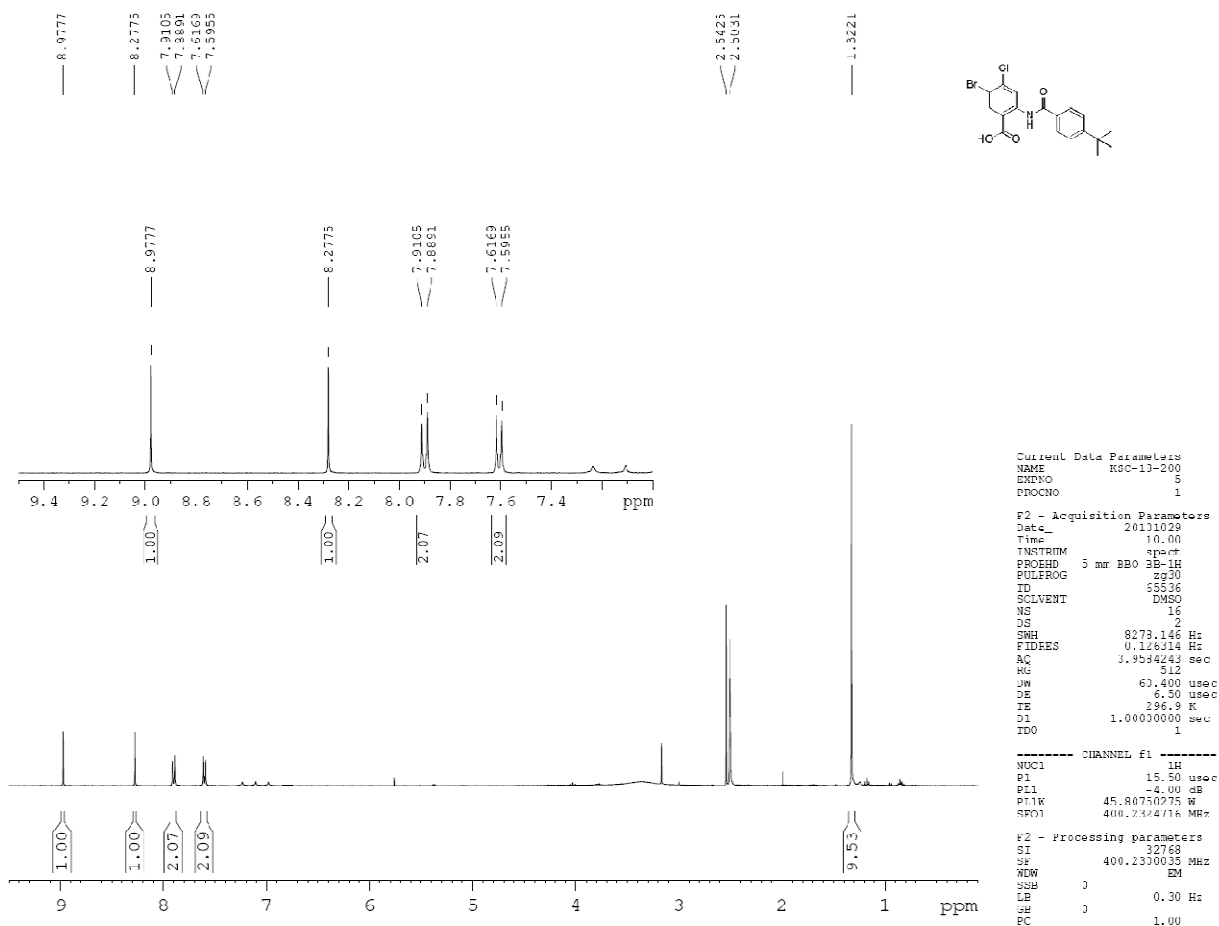


Figure 3. Proton spectra for ML205, SID 99437306, CID 46931017

ML205, SID 99437306, CID 46931017 PROTON NMR DATA: ^1H NMR (400 MHz, DMSO- d_6) δ 13.27 (s, 1H), 8.98 (s, 1H), 8.28 (s, 1H), 7.90 (d, J = 8.5 Hz, 2H), 7.60 (d, J = 8.6 Hz, 2H), 1.32 (s, 9H).

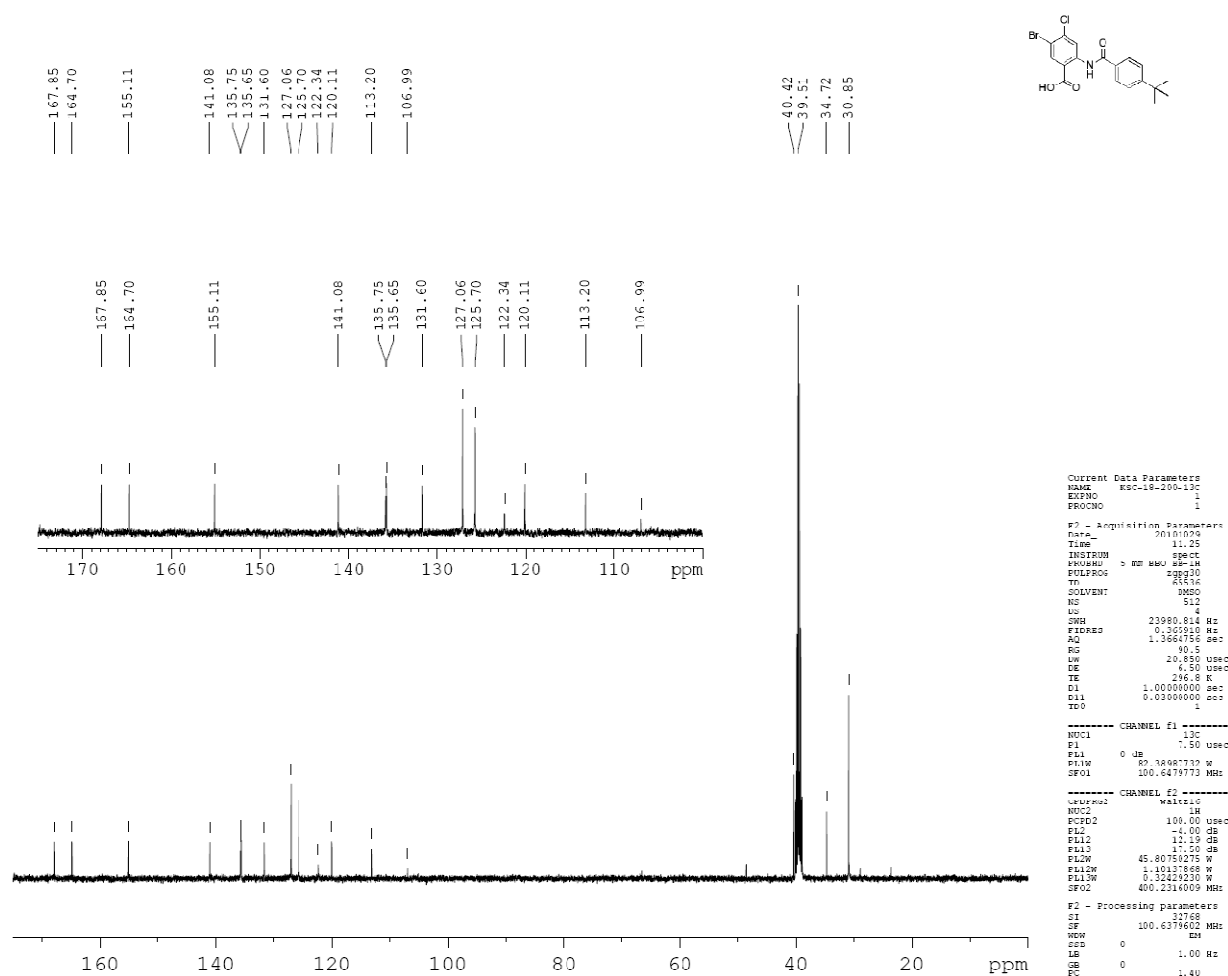
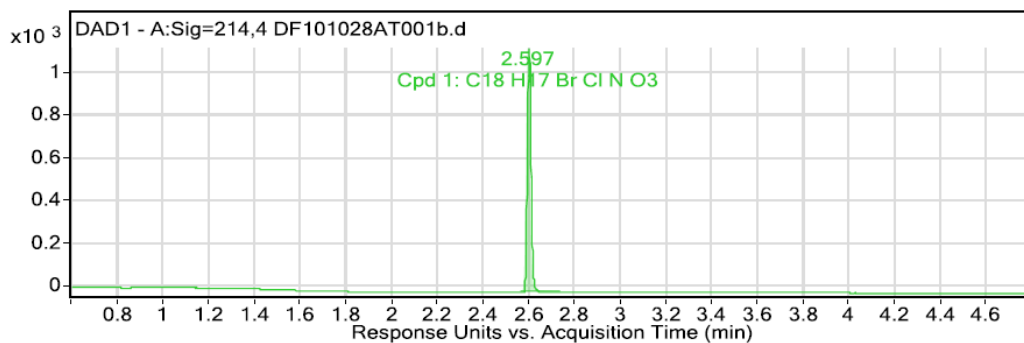


Figure 4. Carbon spectra for ML205, SID 99437306, CID 46931017

ML205, SID 99437306, CID 46931017 CARBON NMR DATA: ^{13}C NMR (100 MHz, DMSO-d_6) δ 167.9, 164.7, 155.1, 141.1, 135.8, 135.7, 131.6, 127.1, 125.7, 122.3, 120.0, 113.2, 34.7, 30.9.

LCMS and HRMS data for ML205, SID 99437306, CID 46931017: Detailed analytical methods and instrumentation are described in section 2.3, entitled “Probe Preparation” under general experimental and analytical details. The numerical experimental LCMS and HRMS data are represented below, along with the associated spectra.



User Chromatogram Peak List

Peak #	Compound Name	RT	Height	Height %	Area	Area %	Area Sum %	Width
1	Cpd 1: C18 H17 Br Cl N O3	2.597	1119.43	100	1266.12	100	100	0.017

Figure 5. LCMS purity data at 215 nm for ML205, SID 99437306, CID 46931017; LCMS retention time: 2.597 min; purity at 215 nm = 100%.

Compound Label	RT	Mass	Abund	Formula	Tot Mass	Purity Value
Cpd 1: C18 H17 Br Cl N O3	2.592	409.0089	191057	C18 H17 Br Cl N O3	409.008	100

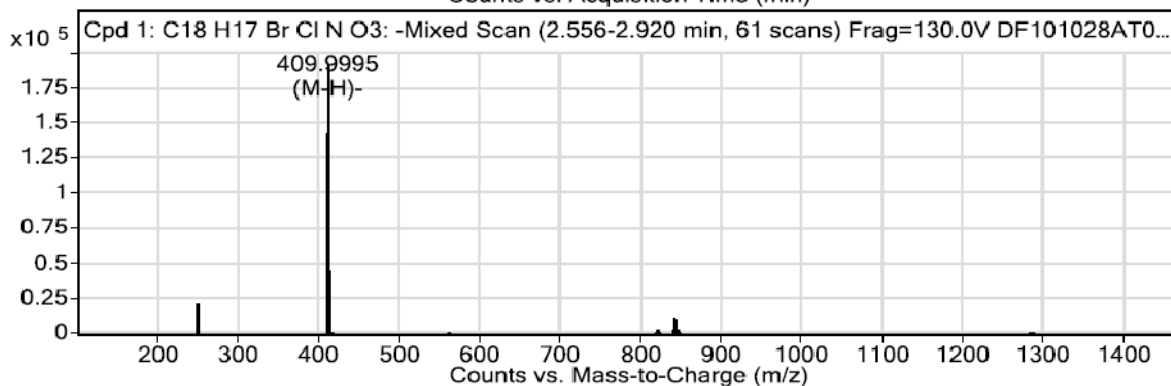
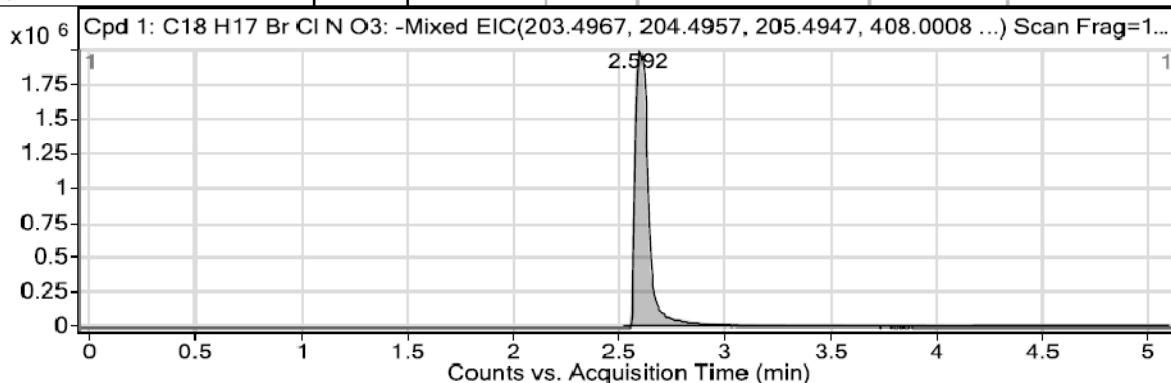


Figure 6. HRMS data for ML205, SID 99437306, CID 46931017; HRMS m/z calculated for $C_{18}H_{17}BrClNO_3 [M^+ - 1]$ 410.69, found 409.9995.

C. Solubility:

Aqueous solubility was measured in phosphate buffered saline (PBS) at room temperature (23°C). PBS by definition is 137 mM NaCl, 2.7 mM KCl, 10 mM sodium phosphate dibasic, 2 mM potassium phosphate monobasic and a pH of 7.4. The

solubility of probe ML205, SID 99437306, CID 46931017 was determined to be 25.6 $\mu\text{g/mL}$ [12].

D. Stability:

Stability was measured at room temperature (23°C) in PBS (no antioxidants or other protectants and DMSO concentration below 0.1%). The stability of probe compound ML205, SID 99437306, CID 46931017, determined as the percent of compound remaining after 48 hours, was 100% [12].

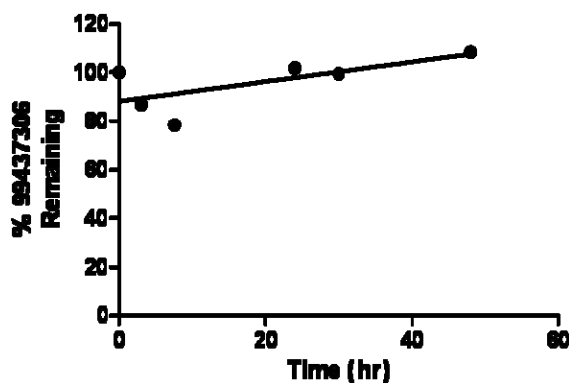
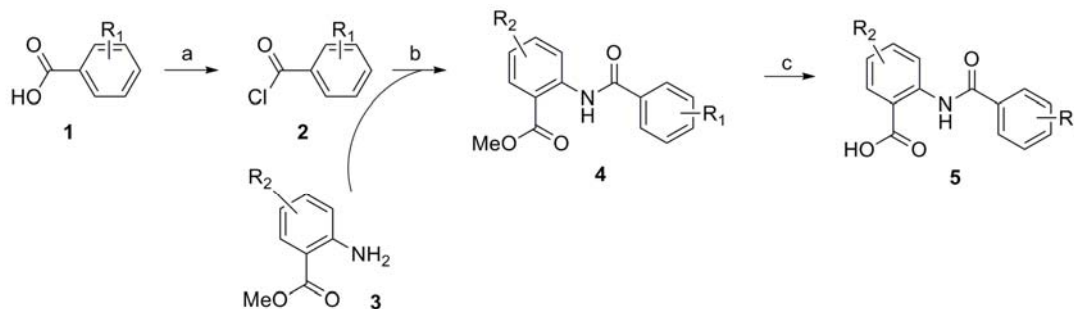


Figure 7. Stability data depicted as a graph showing the loss of ML205 with time over a 48 hr period. The probe appears to be stable under the experimental conditions, as the percent of compound remaining was 100%.

E. Synthetic Route:

The probe and analogs were generally synthesized by the method shown (Fig. 8). Commercial acid chlorides were used when available. Otherwise, substituted benzoic acids **1** were converted to the corresponding acid chlorides **2** using oxalyl chloride. The crude acid chlorides were then treated with substituted aminobenzoates **3** in the presence of pyridine to afford amidobenzoates **4**. Hydrolysis of the carboxylic esters provided the desired acids **5**. Specific experimental details for the probe are detailed in section 2.3 below, entitled, "Probe Preparation."



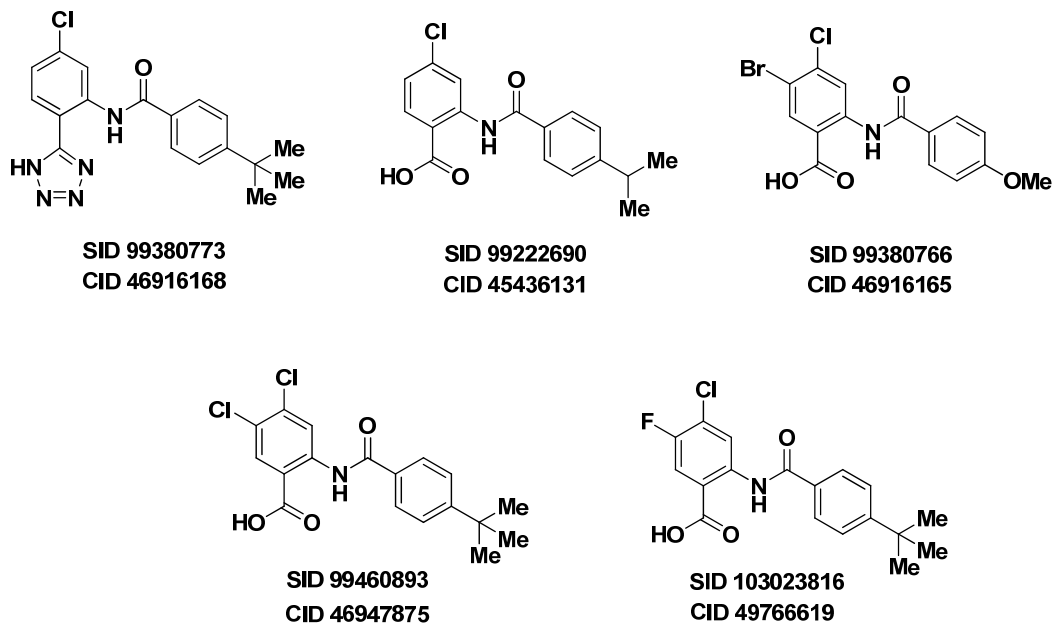
Reagents: (a) (COCl)₂, DMF, DCM, 0 °C to rt, 2h; (b) pyridine, THF, 50 °C, 18 h; (c) LiOH, THF/H₂O, rt, 3h.

Figure 8. General synthetic route for probe and analogue synthesis

If a requisite substituted benzoic acid or acid chloride was unavailable, the desired intermediates were prepared by Molander-type coupling of a halogenated benzoate or by Friedel-Crafts alkylation of the appropriate benzoate [13, 14].

F. Submission of Five Related Analogues to the MLSMR:

Five analogues have been fully characterized and prepared in sufficient quantity for submission to the MLSMR. The five selected analogs and associated data are shown in Figure 9.



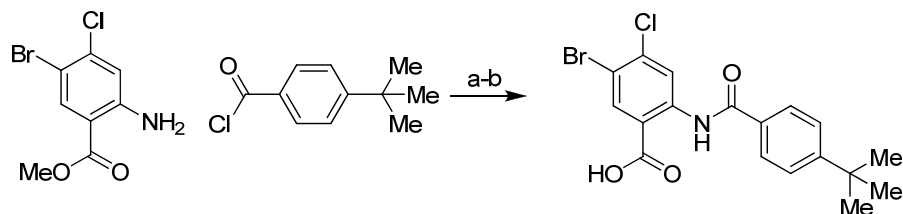
Entry	SID	CID	TbHK1 IC ₅₀ μM	G6PDH IC ₅₀ μM	IMR90 EC ₅₀ μM	hGik % inhibition at 10 μM	BSF % inhibition at 10 μM
1	99380773	46916168	3.46	> 25	> 25	28.4	29 ± 6
2	99222690	45436131	2.89	> 25	> 25	0	34 ± 10
3	99380766	46916165	4.59	> 25	> 25	22.3	43 ± 12
4	99460893	46947875	1.36	> 25	> 25	0	35 ± 11
5	103023816	49766619	2.79	> 25	> 25	0	32 ± 11

Figure 9. Five analogues selected for submission to support probe ML205, SID 99437306, CID 46931017 and associated data.

2.3 Probe Preparation

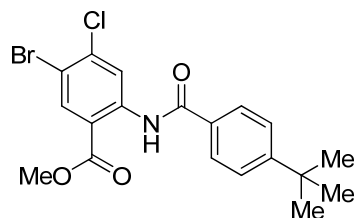
General experimental and analytical details: ¹H and ¹³C NMR spectra were recorded on a Bruker AM 400 spectrometer (operating at 400 and 101 MHz respectively) in CDCl₃ with 0.03% TMS as an internal standard or DMSO-d₆. The chemical shifts (δ) reported are given in parts per million (ppm) and the coupling constants (J) are in Hertz (Hz). The spin multiplicities are reported as s = singlet, br. s = broad singlet, d = doublet, t = triplet, q = quartet, dd = doublet of doublet and m = multiplet. The LCMS analysis was performed on an Agilent 1200 RRL chromatograph with photodiode array UV detection and an Agilent 6224 TOF mass spectrometer. The chromatographic method utilized the following parameters: a Waters Acquity BEH C-18 2.1 x 50mm, 1.7 μm column; UV detection wavelength = 214 nm; flow rate = 0.4ml/min; gradient = 5 - 100% acetonitrile over 3 minutes with a hold of 0.8 minutes at 100% acetonitrile; the aqueous mobile phase contained 0.15% ammonium hydroxide (v/v). The mass spectrometer utilized the following parameters: an Agilent multimode source which simultaneously acquires ESI+/APCI+; a reference mass solution consisting of purine and hexakis(1H, 1H, 3H-tetrafluoropropoxy) phosphazine; and a make-up solvent of 90:10:0.1 MeOH:Water:Formic Acid which was introduced to the LC flow prior to the source to assist ionization. The melting point was determined on a Stanford Research Systems OptiMelt apparatus.

Probe compound MI205, SID 99437306, CID 46931017 was prepared by coupling 2-amino-5-bromo-4-chlorobenzoate with 4-*tert*-butylbenzoyl chloride, followed by hydrolysis (Figure 10).



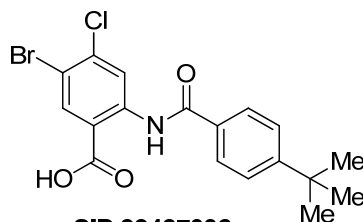
Reagents: a) pyridine, THF, 50 °C, 18 h, 68%; b) LiOH, THF/H₂O, rt, 3 h, 93%.

Figure 10. Assembly of probe compound ML205, SID 99437306, CID 46931017



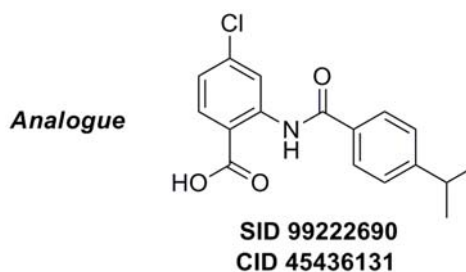
Methyl 2-(4-*tert*-butylbenzamido)-5-bromo-4-chlorobenzoate. Methyl 2-amino-5-bromo-4-chlorobenzoate (Ace Synthesis, CAS # 765211-09-4) and 4-*tert*-butylbenzoyl chloride (Sigma-Aldrich, CAS # 1710-98-1) were obtained commercially. In a 40 mL vial was combined sequentially methyl 2-amino-5-bromo-4-chlorobenzoate (0.21 g, 0.81 mmol, 1 eq.), 4-*tert*-butylbenzoyl chloride (0.22 mL, 1.21 mmol, 1.5 eq.) and pyridine (0.098 mL, 1.21 mmol, 1.5 eq.) in THF (2 mL). The resulting colorless solution was stirred under nitrogen at 50 °C for 18 hours. The reaction was removed from heat, cooled to rt, diluted with EtOAc (5 mL) and quenched with saturated aqueous NaHCO₃ (5 mL). After extracting with EtOAc (2 x 5 mL), the crude material was adsorbed onto silica. Purification by silica gel chromatography (0-25% EtOAc:Hex ramp over 20 min) afforded the desired product methyl 2-(4-*tert*-butylbenzamido)-5-bromo-4-chlorobenzoate as a white solid (0.26 g, 0.55 mmol, 68% yield). ¹H NMR (400 MHz, CDCl₃) δ 11.95 (s, 1H), 9.22 (s, 1H), 8.31 (s, 1H), 7.96 (d, *J* = 8.6 Hz, 2H), 7.55 (d, *J* = 8.6 Hz, 2H), 3.99 (s, 3H), 1.36 (s, 9H).

Probe

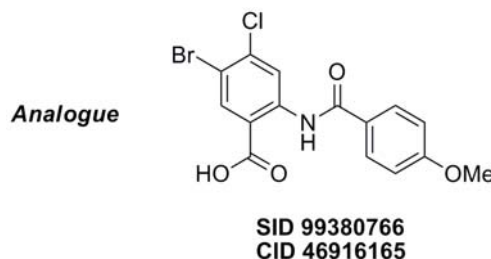


SID 99437306
CID 46931017
ML205

PROBE: 2-(4-*tert*-butylbenzamido)-5-bromo-4-chlorobenzoic acid. (ML205, SID 99437306, CID 46931017): To a mixture of methyl 2-(4-*tert*-butylbenzamido)-5-bromo-4-chlorobenzoate (0.26 g, 0.55 mmol, 1 eq.) and LiOH (0.092 g, 3.84 mmol, 7 eq.) in water (2 mL) was added THF (2 mL) to give a colorless solution. After stirring the solution for 3 h at rt, the reaction was acidified with 1.0 M aq. HCl to pH 2 – 3 and then extracted with CH₂Cl₂ (2 x 5 mL). The separated organic extracts were combined, dried (MgSO₄), filtered and concentrated to produce the desired 2-(4-*tert*-butylbenzamido)-5-bromo-4-chlorobenzoic acid as a white solid (0.23 g, 0.57 mmol, 93 % yield). ¹H NMR (400 MHz, DMSO-d₆) δ 13.27 (s, 1H), 8.98 (s, 1H), 8.28 (s, 1H), 7.90 (d, *J* = 8.5 Hz, 2H), 7.60 (d, *J* = 8.6 Hz, 2H), 1.32 (s, 9H). ¹³C NMR (100 MHz, DMSO-d₆) δ 167.9, 164.7, 155.1, 141.1, 135.8, 135.7, 131.6, 127.1, 125.7, 122.3, 120.0, 113.2, 34.7, 30.9. LCMS retention time: 2.592 min, purity at 215 nm = 100%. HRMS *m/z* calculated for C₁₈H₁₇BrClNO₃ [M⁺ - 1] 410.69, found 409.99. White solid, mp 273 - 276 °C.

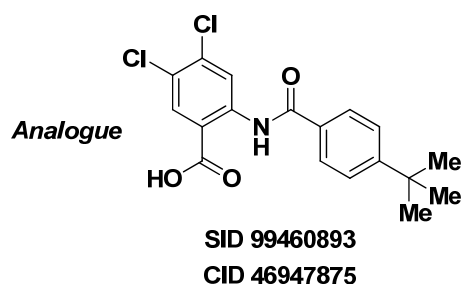


ANALOGUE 1: 4-chloro-2-(4-isopropylbenzamido)benzoic acid (SID 99222690/ CID 45436131): Isolated 42 mg, yield 97% of 4-chloro-2-(4-isopropylbenzamido)benzoic acid as a white solid. ¹H NMR (400 MHz, DMSO-d₆) δ 12.24 (s, 1H), 8.84 (d, *J* = 2.1 Hz, 1H), 8.06 (d, *J* = 8.6 Hz, 1H), 7.88 (d, *J* = 8.4 Hz, 2H), 7.48 (d, *J* = 8.3 Hz, 2H), 7.27 (dd, *J*₁ = 8.6 Hz, *J*₂ = 2.2 Hz, 1H), 2.99 (m, *J* = 6.9 Hz, 1H), 1.24 (d, *J* = 7.0 Hz, 6H). ¹³C NMR (125 MHz, DMSO-d₆) δ 169.37, 164.89, 153.33, 142.28, 138.73, 133.00, 131.66, 127.24, 127.04, 122.72, 119.06, 115.03, 33.43, 23.55. LCMS retention time: 2.327 min, purity at 215 nm = 98.2%. HRMS *m/z* calculated for C₁₇H₁₆ClNO₃ [M⁺ + 1] 317.0818, found 318.0891. White solid, mp 217 – 220 °C.

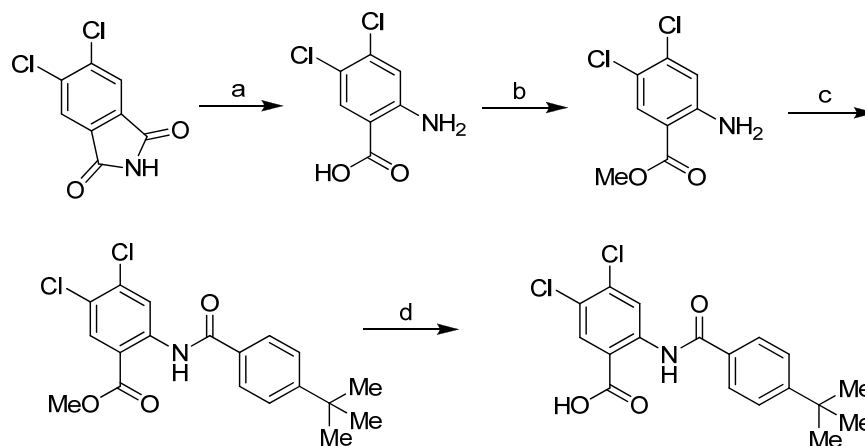


ANALOGUE 2: 5-bromo-4-chloro-2-(4-methoxybenzamido)benzoic acid (SID 99380766/ CID 46916165): Isolated 132 mg, yield 98 % of 5-bromo-4-chloro-2-(4-

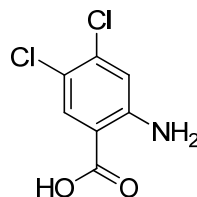
methoxybenzamido)benzoic acid as a white solid. ^1H NMR (400 MHz, DMSO- d_6) δ 12.10 (s, 1H), 8.98 (s, 1H), 8.26 (s, 1H), 7.90 (d, J = 8.8 Hz, 2H), 7.13 (d, J = 8.8 Hz, 2H), 3.86 (s, 3H). ^{13}C NMR (125 MHz, DMSO- d_6) δ 168.22, 164.38, 162.63, 141.22, 138.48, 135.48, 129.08, 125.82, 120.81, 117.02, 114.35, 113.77, 55.56. LCMS retention time: 2.345 min; purity at 215 nm = 100%. HRMS m/z calculated for $\text{C}_{18}\text{H}_{18}\text{ClNO}_3$ [$\text{M}^+ + 1$] 382.9565, found 383.9633. White solid, mp 258 – 261 °C.



ANALOGUE 3: 2-(4-*tert*-butylbenzamido)-4,5-dichlorobenzoic acid. (SID 99437306/ CID 46947875) was prepared according to the following scheme:

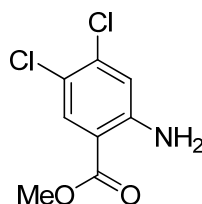


Reagents: a) NaOH, NaOCl, MeOH, 80 °C, 2 h, 60%; b) 4-*tert*-butylbenzoyl chloride, TMS-diazomethane, $\text{CH}_2\text{Cl}_2/\text{MeOH}$, rt, 30 min, 87%; c) CH_3CN , 150 °C, 30 min, MW, 32%; d) LiOH, THF/ H_2O , rt, 3 h, 96%.

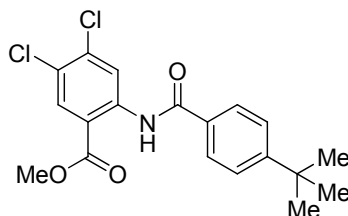


2-Amino-4,5-dichlorobenzoic acid. The starting material 4,5-dichlorophthalimide (CAS# 15997-89-4) was purchased from Sigma-Aldrich. In a vial was added the 4,5-dichlorophthalimide (1.93 g, 8.92 mmol, 1 eq.) and MeOH (10 mL). The 10.0 M NaOH (3.6 mL, 35.6 mmol, 4 eq.) and 10 % w/w NaOCl solution (6.08 mL, 9.81

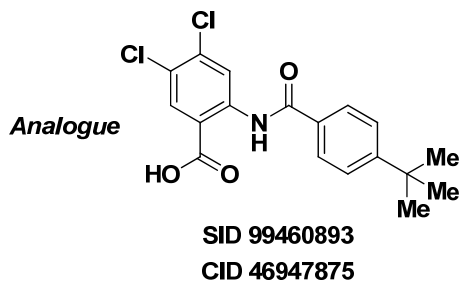
mmol, 1.1 eq) were added and the reaction stirred for 2 hours at 80 °C. The reaction was then cooled to rt and was poured into 220 mL of 1.0 M HCl. After extracting with CHCl₃ (3 x 200 mL) the crude material was adsorbed onto silica. Purification by silica gel chromatography (0-100% EtOAc:Hex ramp over 20 min) afforded the desired product 2-amino-4,5-dichlorobenzoic acid as a white solid (1.09 g, 5.30 mmol, 60% yield). ¹H NMR (400 MHz, DMSO-d₆) δ 7.77 (s, 1H), 7.10 (s, 1H).



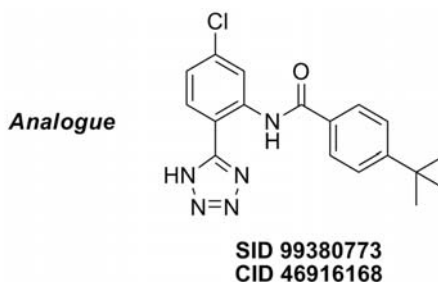
Methyl 2-amino-4,5-dichlorobenzoate. To a vial was added 2-amino-4,5-dichlorobenzoic acid (0.66 g, 3.21 mmol, 1 eq.) and DCM/MeOH (3 mL/2 mL). A solution of 2.0 M TMS-diazomethane in hexanes (2.89 mL, 5.78 mmol, 1.8 eq.) was added dropwise and the reaction stirred for 30 minutes at rt. The crude material was then adsorbed onto silica. Purification by silica gel chromatography (0-20% EtOAc:Hex ramp over 20 min) afforded the desired product methyl 2-amino-4,5-dichlorobenzoate as a white solid (0.61 g, 2.80 mmol, 87% yield). ¹H NMR (400 MHz, CDCl₃) δ 7.92 (s, 1H), 7.79 (s, 1H), 5.77 (brs, 2H), 3.87 (s, 3H).



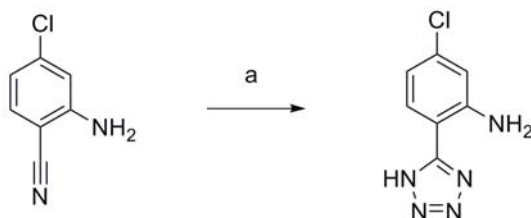
Methyl 2-(4-*tert*-butylbenzamido)-4,5-dichlorobenzoate. To a microwave vial was added the methyl 2-amino-4,5-dichlorobenzoate (0.11 g, 0.48 mmol, 1 eq.), 4-*tert*-butylbenzoyl chloride (CAS# 1710-98-1) (0.096 mL, 0.527 mmol, 1.1 eq.) and MeCN (2.0 mL). The vial was sealed and the reaction stirred in a microwave at 150 °C for 30 minutes. The reaction was then cooled to rt and was diluted with EtOAc (10 mL) and washed with saturated NaHCO₃ (10 mL). The crude material was then adsorbed onto silica. Purification by silica gel chromatography (0-15% EtOAc:Hex ramp over 10 min) afforded the desired product methyl 2-(4-*tert*-butylbenzamido)-4,5-dichlorobenzoate as a white solid (0.059 g, 0.16 mmol, 32% yield). ¹H NMR (400 MHz, CDCl₃) δ 11.94 (brs, 1H), 9.22 (s, 1H), 8.15 (s, 1H), 7.96 (d, *J* = 8.6 Hz, 2H), 7.55 (d, *J* = 8.6 Hz, 2H), 3.99 (s, 3H), 1.36 (s, 9H).



ANALOGUE 3: 2-(4-*tert*-butylbenzamido)-4,5-dichlorobenzoic acid. (SID 99437306/ CID 46947875) To a mixture of methyl 2-(4-*tert*-butylbenzamido)-4,5-dichlorobenzoate (0.019 g, 0.050 mmol, 1 eq.) and LiOH (0.010 g, 0.35 mmol, 7 eq.) in water (1 mL) was added THF (1 mL) to give a colorless solution. After stirring the solution for 3 h at rt, the reaction was acidified with 1.0 M aq. HCl to pH 2 – 3 and then extracted with CH₂Cl₂ (2 x 5 mL). The separated organic extracts were combined, dried (MgSO₄), filtered and concentrated to produce the desired 2-(4-*tert*-butylbenzamido)-4,5-dichlorobenzoic acid as a white solid (0.017 g, 0.048 mmol, 96% yield). ¹H NMR (400 MHz, DMSO-*d*₆) δ 12.17 (brs, 1H), 9.00 (s, 1H), 8.16 (s, 1H), 7.88 (d, *J* = 8.6 Hz, 2H), 7.63 (d, *J* = 8.6 Hz, 2H), 1.33 (s, 9H). ¹³C NMR (125 MHz, DMSO-*d*₆) δ 168.2, 164.9, 155.7, 140.6, 136.4, 132.4, 131.0, 127.0, 126.0, 124.5, 121.1, 117.2, 34.8, 30.9. LCMS retention time: 2.514 min; Purity at 215 nm = 97.9%. HRMS *m/z* calculated for C₁₈H₁₇Cl₂NO₃ [*M*⁺ - 1] 365.06, found 364.05. White solid, mp 242 - 245 °C.

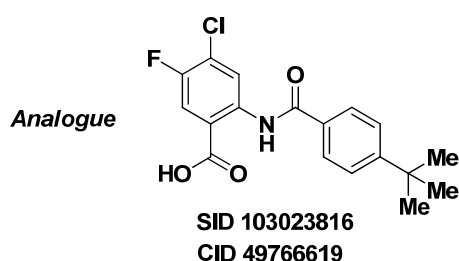


ANALOGUE 4: 4-(*tert*-butyl)-N-(5-chloro-2-(1H-tetrazol-5-yl)phenyl)benzamide (SID 99380773/ CID 46916168): Isolated 67 mg, 61% yield of 4-(*tert*-butyl)-N-(5-chloro-2-(1H-tetrazol-5-yl)phenyl)benzamide as a white solid. ¹H NMR (400 MHz, DMSO-*d*₆) δ 11.73 (s, 1H), 8.78 (d, *J* = 2.2 Hz, 1H), 8.04 (d, *J* = 8.5 Hz, 1H), 8.02 – 7.96 (m, 2H), 7.67 – 7.60 (m, 2H), 7.45 (dd, *J* = 8.5, 2.2 Hz, 1H), 1.34 (s, 9H). ¹³C NMR (101 MHz, DMSO-*d*₆) δ 165.12, 155.47, 138.43, 136.25, 131.18, 129.98, 127.21, 125.77, 123.77, 120.63, 111.64, 97.71, 34.78, 30.83. LCMS retention time: 2.514 min; LCMS purity at 215 nm = 100%. HRMS *m/z* calculated for C₁₈H₁₈ClN₅O [*M*⁺+1]: 356.1273, found 356.1264. White solid, mp 231-234 °C.

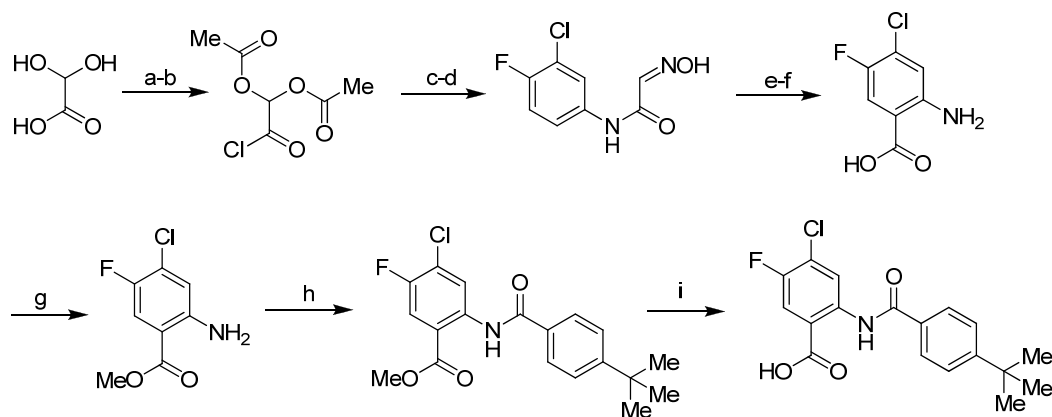


Reagents: (a) NaN_3 , $\text{Et}_3\text{N}\cdot\text{HCl}$, PhMe, MWI, 110 °C

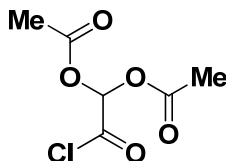
The requisite 5-chloro-2-(1H-tetrazol-5-yl)aniline precursor to analogue 4 (CID 46916168; SID 99380773) was prepared according to a previously reported procedure [15].



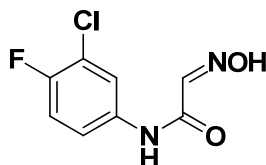
ANALOGUE 5: 2-(4-tert-butylbenzamido)-4-chloro-5-fluorobenzoic acid (SID 103023816/ CID 49766619): This analogue was prepared according to the scheme shown below:



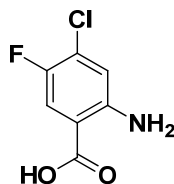
Reagents and conditions: a) acetic anhydride, acetic acid, reflux, 2 h; b) SOCl_2 , CH_2Cl_2 , 45 °C for 2 h, 51% for two steps; c) 3-chloro-4-fluoroaniline, KHCO_3 , CH_2Cl_2 , -10 °C - rt, 20 h; d) hydroxylamine-HCl, $\text{EtOH}/\text{H}_2\text{O}$, reflux, 2 h, 45% for two steps; e) H_2SO_4 , 80 °C, 3 h; f) NaOH , H_2O_2 , 80 °C, 3 h, 54% for two steps; g) TMS-diazomethane, $\text{CH}_2\text{Cl}_2/\text{MeOH}$, rt, 30 min, 82%; h) 4-*tert*-butylbenzoyl chloride, CH_3CN , 150 °C, 50 min, MW, 56%; i) LiOH , $\text{THF}/\text{H}_2\text{O}$, rt, 3 h, 94%.



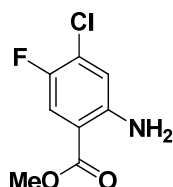
2,2-diacetoxyacetyl chloride. The requisite starting materials glyoxylic acid monohydrate was purchased from Sigma-Aldrich (CAS # 563-96-2). To a vial was added glyoxylic acid monohydrate (2.05 g, 22.3 mmol, 1 eq.), acetic anhydride (21.0 mL, 223 mmol, 10 eq.) and acetic acid (5 mL). The colorless mixture was heated under reflux for 2 hr. The reaction was then cooled to rt, and the solvents were removed by rotary evaporation. The remaining volatiles were azeotroped with toluene and the crude material was solubilized in CH₂Cl₂. Thionyl chloride (5.68 mL, 78.1 mmol, 3.5 eq.) was added to the mixture and the reaction stirred at 45 °C for 2 hr. The reaction was cooled to rt, the volatiles were removed by rotary evaporation and the remaining material was isolated as the desired product, 2,2-diacetoxyacetyl chloride, as a brown oil (2.21 g, 11.4 mmol, 51% yield). ¹H NMR (400 MHz, CDCl₃) δ 6.89 (s, 1H), 2.19 (s, 6H).



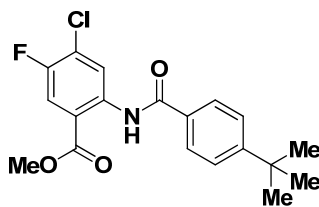
N-(3-chloro-4-fluorophenyl)-2-(hydroxyimino)acetamide. The requisite starting material 3-chloro-4-fluoroaniline was purchased from Sigma-Aldrich (CAS # 367-21-5). To a vial was added the 3-chloro-4-fluoroaniline (2.71 g, 18.6 mmol, 1 eq.), potassium hydrogen-carbonate (9.31 g, 93.0 mmol, 5 eq.) in CH₂Cl₂ (35 mL), and the reaction was cooled to -10 °C. The 2,2-diacetoxyacetyl chloride (4.69 g, 24.2 mmol, 1.3 eq.) in CH₂Cl₂ (15 mL) was added dropwise and the reaction was allowed to warm to rt and stirred for 20 h. The reaction was filtered and rinsed with CH₂Cl₂ and the filtrate was concentrated. The crude material was then dissolved in EtOH:H₂O (50 mL:20 mL) and hydroxylamine-HCl (6.46 g, 93.0 mmol, 5 eq.) was added. The reaction stirred at reflux for 2 hr, cooled to rt, and the EtOH was removed by rotary evaporation to form a precipitate. The solid was filtered and rinsed with water (50 mL) and dried on the filter to produce N-(3-chloro-4-fluorophenyl)-2-(hydroxyimino)acetamide as an off-white solid (1.83 g, 8.43 mmol, 45% yield). ¹H NMR (400 MHz, CDCl₃) δ 12.25 (s, 1H), 10.38 (s, 1H), 7.99 (dd, *J*₁ = 6.8 Hz, *J*₂ = 2.6 Hz, 1H), 7.65 – 7.60 (m, 2H), 7.40 (t, *J* = 9.1 Hz, 1H).



2-Amino-4-chloro-5-fluorobenzoic acid. To a vial was added the N-(3-chloro-4-fluorophenyl)-2-(hydroxyimino)acetamide and concentrated sulfuric acid (30 mL). The reaction then stirred for 3 hr at 80°C, cooled to rt and poured onto ice. The product was extracted with CHCl₃ (3 x 200 mL) and the organic layers were combined and concentrated by rotary evaporation. The crude material was solubilized in aqueous 2.5 M NaOH (20 mL), 30 % w/w hydrogen peroxide (2.50 mL, 24.3 mmol, 3 eq.) was added and the reaction stirred at 80°C for 3 h, cooled to rt and was acidified carefully with concentrated HCl to pH 3. The resulting precipitate was filtered and rinsed with water to produce 2-amino-4-chloro-5-fluorobenzoic acid as a reddish-brown solid (0.86 g, 4.60 mmol, 54% yield). ¹H NMR (400 MHz, DMSO-d₆) δ 7.55 (d, *J* = 10.3 Hz, 1H), 6.93 (d, *J* = 6.5 Hz, 2H).

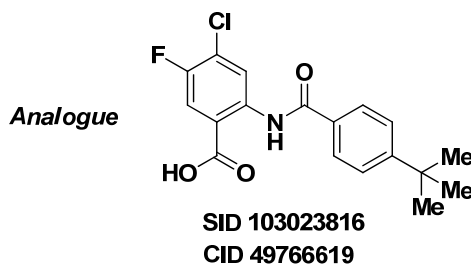


Methyl 2-amino-4-chloro-5-fluorobenzoate. To a vial was added 2-amino-4-chloro-5-fluorobenzoic acid (0.046 g, 0.24 mmol, 1 eq.) and CH₂Cl₂/MeOH (3 mL/2 mL). A solution of 2.0 M TMS-diazomethane in hexanes (0.22 mL, 0.44 mmol, 1.8 eq.) was added dropwise, and the reaction stirred for 30 minutes at rt. The crude material was then adsorbed onto silica. Purification by silica gel chromatography (0-20% EtOAc:Hex ramp over 20 min) afforded the desired product methyl 2-amino-4-chloro-5-fluorobenzoate as a white solid (0.041 g, 0.20 mmol, 82 % yield). ¹H NMR (400 MHz, CDCl₃) δ 7.62 (d, *J* = 9.8 Hz, 1H), 6.71 (d, *J* = 6.1 Hz, 1H), 3.87 (s, 3H).



Methyl 2-(4-tertbutylbenzamido)-4-chloro-5-fluorobenzoate. To a microwave vial was added the methyl 2-amino-4-chloro-5-fluorobenzoate (0.076 g, 0.37 mmol, 1 eq.), 4-*tert*-butylbenzoyl chloride (CAS# 1710-98-1) (0.082 mL, 0.45 mmol, 1.2 eq.) and MeCN (2.0 mL). The vial was sealed and the reaction stirred in a microwave at 150 °C for 50 minutes. The reaction was then cooled to rt and was diluted with EtOAc (10 mL) and washed with saturated aqueous NaHCO₃ (10 mL). The crude material was then adsorbed onto silica. Purification by silica gel chromatography (0-15% EtOAc:Hex ramp over 10 min) afforded the desired product methyl 2-(4-tertbutylbenzamido)-4-chloro-5-fluorobenzoate as a white solid (0.076 g, 0.21 mmol, 56% yield). ¹H NMR (400 MHz, CDCl₃) δ 11.89 (s, 1H), 9.17

(d, $J = 7.1$ Hz, 1H), 7.96 (d, $J = 8.7$ Hz, 2H), 7.84 (d, $J = 9.5$ Hz, 1H), 7.55 (d, $J = 8.6$ Hz, 2H), 3.98 (s, 3H), 1.36 (s, 9H).



ANALOGUE 5: 2-(4-tert-butylbenzamido)-4-chloro-5-fluorobenzoic acid (SID 103023816/ CID 49766619): To a mixture of methyl 2-(4-tertbutylbenzamido)-4-chloro-5-fluorobenzoate (0.076 g, 0.21 mmol, 1 eq.), and LiOH (0.035 g, 1.5 mmol, 7 eq.) in water (2 mL) was added THF (2 mL) to give a colorless solution. After stirring the solution for 3 h at rt, the reaction was acidified with 1.0 M aq. HCl to pH 2 – 3 and then extracted with CH₂Cl₂ (2 x 5 mL). The separated organic extracts were combined, dried (MgSO₄), filtered and concentrated to produce the desired 2-(4-tertbutylbenzamido)-4-chloro-5-fluorobenzoic acid as a white solid (0.069 g, 0.196 mmol, 94% yield). ¹H NMR (400 MHz, DMSO-d₆) δ 12.06 (s, 1H), 8.92 (d, $J = 7.08$ Hz, 1H), 7.96 (d, $J = 9.8$ Hz, 1H), 7.88 (d, $J = 8.6$ Hz, 2H), 7.62 (d, $J = 8.6$ Hz, 2H), 1.33 (s, 9H). ¹³C NMR (125 MHz, DMSO-d₆) δ 168.3, 164.7, 155.5, 152.0 (d, $J = 244.1$ Hz), 138.1 (d, $J = 2.8$ Hz), 131.1, 127.0, 125.9, 125.0 (d, $J = 18.1$ Hz), 121.4, 118.5 (d, $J = 23.0$ Hz), 117.3 (d, $J = 5.6$ Hz), 34.8, 30.9. LCMS retention time = 3.641 min; purity at 215 nm = 98.3%. HRMS m/z calculated for C₁₈H₁₇ClFNO₃ [M⁺ - 1] 349.09, found 350.09. White solid, mp 250 – 252 °C.

3 Results

The HTS effort produced three distinct scaffolds for possible development. Each of these was pursued with varying results, described in more detail below. However, one scaffold was amenable to optimization and was evaluated according to the flow chart in Figure 11. Based on knowledge of prior art, probe criteria was established as a compound showing rTbHK1 inhibition of ≤ 1 μ M and not interfering with the reporter enzyme G6PDH (IC₅₀ > 10x TbHK1 IC₅₀). During the course of the project, the team agreed that assessment of the compounds in an IMR90 growth inhibition assay would be valuable, and this criterion was added to those desirable probe characteristics. Additionally, the team also decided to test compounds for potential undesirable cross reactivity, due to inhibition of the related human enzyme, hGlk. While not critical to the probe criteria, the assay provider also agreed to assess compounds in an additional assay for informative purposes to enhance the impact of the probe. Compounds were for evaluated for their ability to inhibit cell growth of *T. brucei* parasites in the bloodstream form cytotoxicity assay.

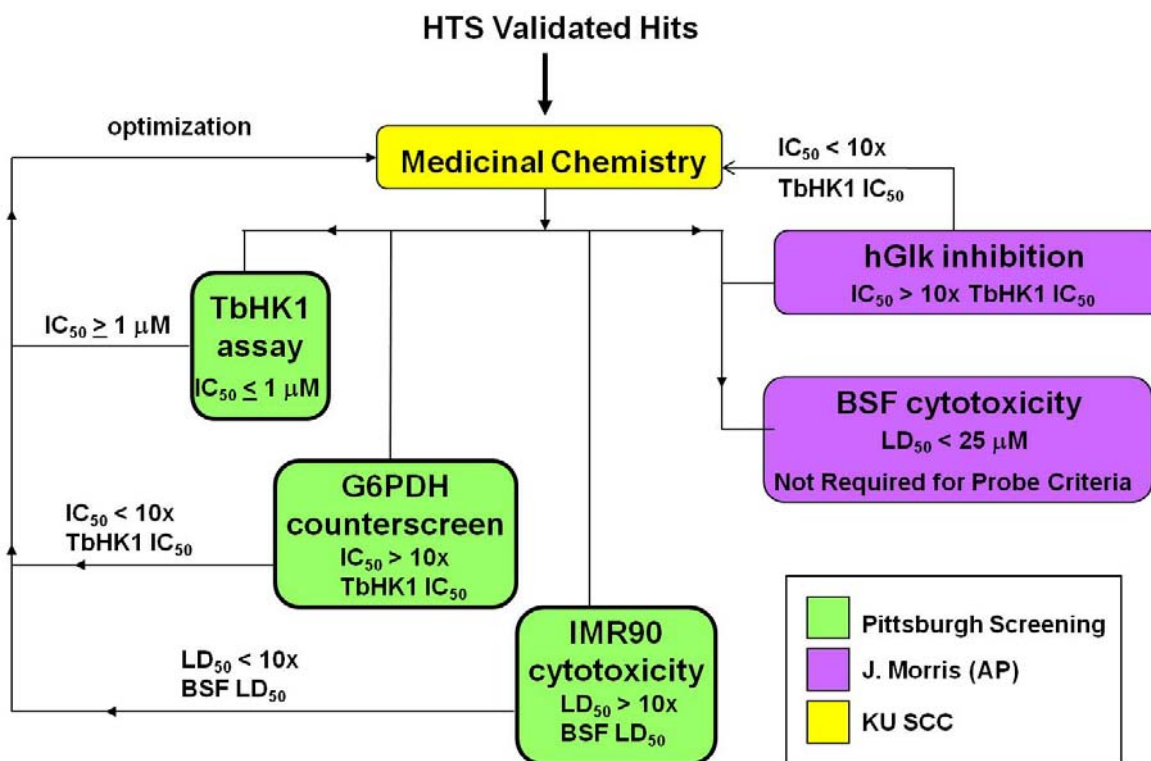


Figure 11. Triage of HTS hits and progression to meet probe criteria.

3.1 Summary of Screening Results

The Pittsburgh Molecular Libraries Screening Center (PMLSC, MLSCN phase) screened 220,223 compounds, available as part of the NIH Molecular Libraries Roadmap Initiative, at a single concentration (10 μM) for small molecule inhibitors of TbHK1 (AID 1430). The TbHK1 coupled assay was optimized and validated for HTS by screening the LOPAC set. Compounds were assayed in duplicate at a single concentration (10 μM) and reproducibility between the duplicate screens is represented in Figure 12A ($R^2 = 0.96$). The HTS assay performed robustly (average Z-factors of 0.80 ± 0.1) and identified 239 compounds as primary actives ($> 50\%$ inhibition at 10 μM), for an overall hit rate of 0.1% (Fig 12B). The 239 active compounds were cherry-picked from DPI (of which 212 were available), and the initial inhibitory activity was confirmed in the primary TbHK1 assay (AID 2560) to afford 29 confirmed compounds. The compounds were then tested against the reporter enzyme, G6PDH, to verify that they did not interfere with the assay format (AID 2516). This effort afforded 16 hit compounds that were then assessed via a 20 point IC_{50} value determination (AID 1632) [7]. These assays are bundled in PubChem under summary AID 2600.

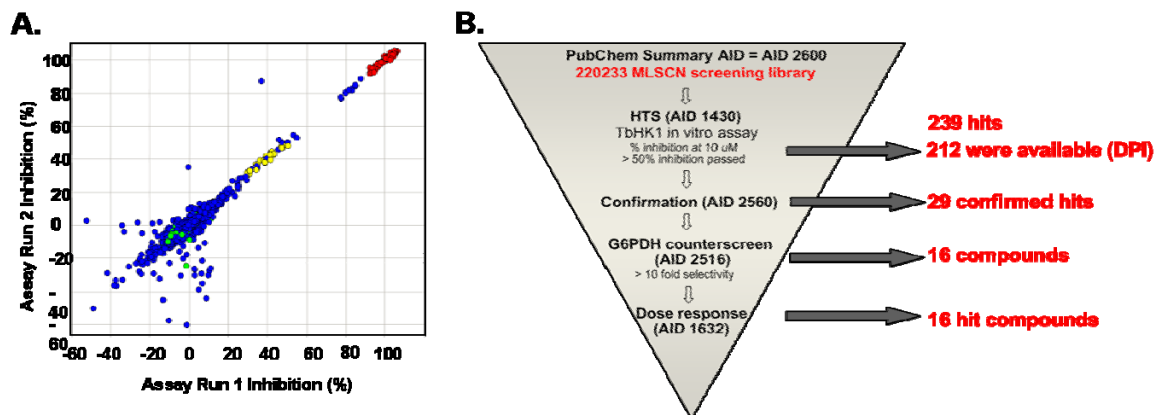


Figure 12. A: plot of percent inhibition for duplicate screen of the 1280 LOPAC screening deck. LOPAC compounds (blue), minimum control, which should equal ~100% inhibition of signal readout (red), IC₅₀ control compounds (yellow), and maximum control compounds, which should equal ~0% inhibition of signal readout (green), are indicated. B. Summary of HTS outcome and hit triage.

Of the 16 hits obtained from the HTS effort, three scaffolds were suitable from the perspective of lacking reactive functionality, being synthetically accessible, and demonstrating a reasonable activity profile (Figure 13).

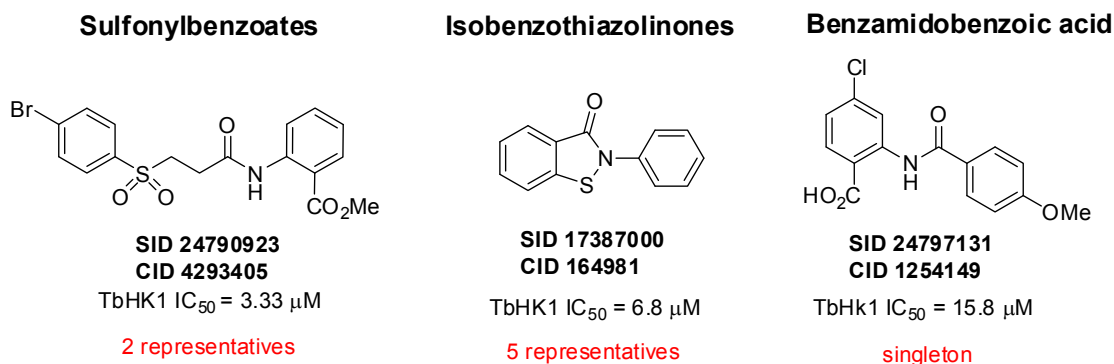


Figure 13. HTS scaffolds and associated data prior to validation from resynthesized solid materials

The two sulfonylbenzoates were resynthesized and upon retest, both compounds failed to confirm. Representatives from the isobenzothiazolinones and the one benzamidobenzoic acid were validated from resynthesized powder material.

3.2 Dose Response Curves for Probe ML205, SID 99437306, CID 46931017

The dose response curves for probe ML205, SID 99437306, CID 46931017 are depicted in Figure 14. The probe demonstrated submicromolar activity versus rTbHK1 (IC₅₀ = 0.98 μ M, Fig. 14B). Probe ML205 (SID 99437306) did not show activity in the IMR90 growth

inhibition assay or the G6PDH counterscreen ($> 25 \mu\text{M}$ for both, Figure 14C and 14D, respectively).

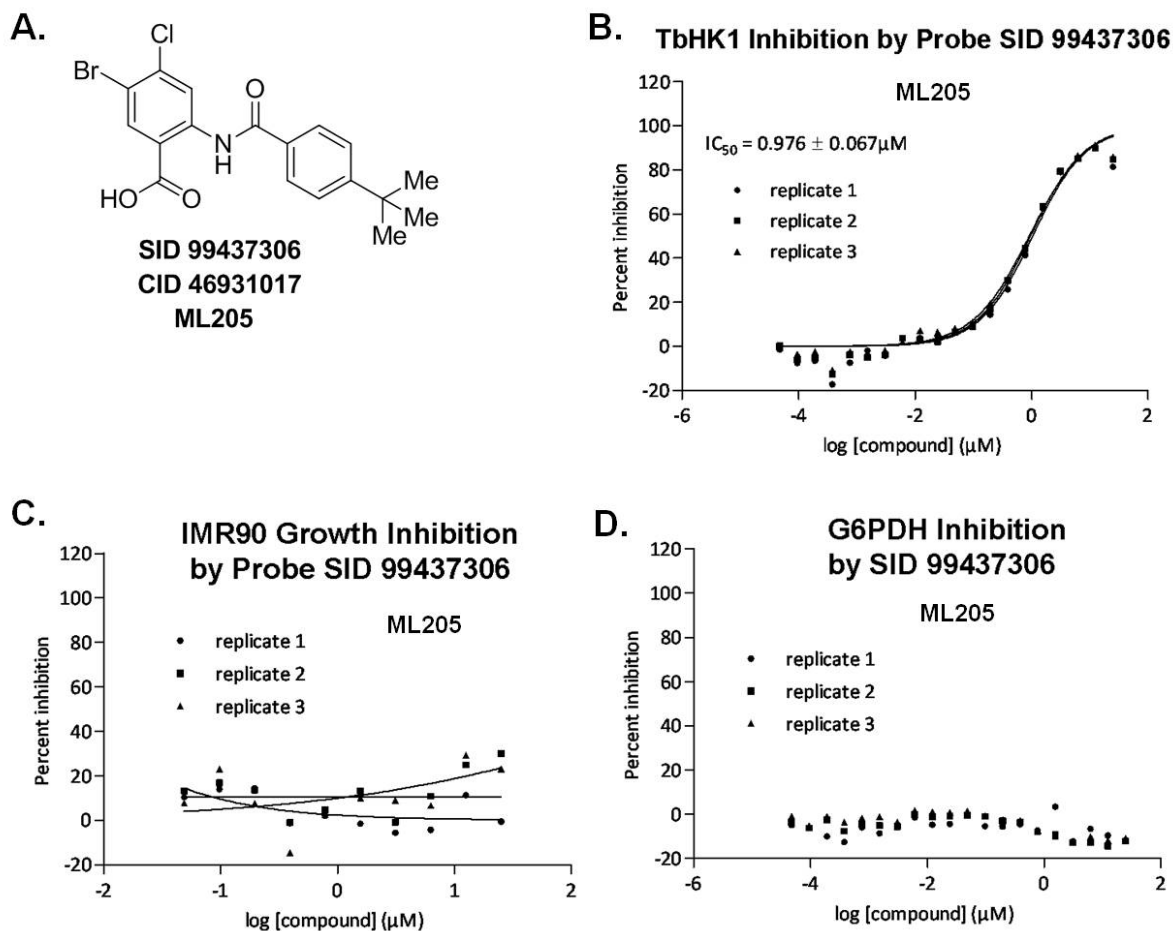


Figure 14. A. probe structure; B. dose response curve for rTbHK1 inhibition by probe ML205, SID 99437306; C. dose response curve for IMR90 growth inhibition by probe – no EC_{50} determined over the concentration range evaluated ($EC_{50} > 25 \mu\text{M}$); D. G6PDH inhibition by probe – no IC_{50} determined over the concentration range evaluated ($IC_{50} > 25 \mu\text{M}$).

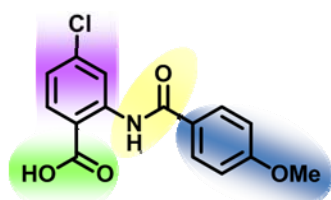
3.3 Scaffold/Moiety Chemical Liabilities

The benzamidobenzoic acid scaffold and its derivatives have been easily handled in terms of stability to reaction conditions, exposure to acid or base, heating, and general manipulation. Most are isolated as stable solid materials. We have not observed decomposition nor have we experienced any chemical liability with these compounds. The structure does not contain moieties that are known generally to be reactive. The stability data that was collected has shown that after 48 hrs, 100% of the starting material remains (see section 2.2D, Figure 7).

3.4 SAR Tables and Discussion

Incipient SAR was observed from the initial HTS set of isobenzothiazolinones (see Figure 13), so a chemistry effort was launched around this primary scaffold (SID 17387000/ CID 164981). Chemistry was developed to support the synthesis of compounds, and a total of 86 compounds were submitted for testing related to SID 17387000. The only clear trend observed with this chemotype was that the presence of the sulfur was necessary for any TbHK1 *in vitro* activity, thus implicating its participation in possible covalent interactions with nucleophilic residues, as we have had experience with this particular chemotype in the context of other projects and shown this to be true. While compounds were identified in the series with improved *in vitro* TbHK1 activity (SID 85285422, TbHK1 IC₅₀ = 1.03 ± 0.17 μM) and lacking G6PDH activity (IC₅₀ > 25 μM), clear SAR trends were difficult to draw out after a rigorous structural modification effort.

These results prompted the team to pursue the singleton benzamidobenzoic acid as a secondary chemotype. Over the course of the pursuing analogs of SID 24798131/CID 1254149, the parent hit has been tested 9 times in triplicate, demonstrating consistent *in vitro* TbHK1 activity on average of IC₅₀ = 9.12 μM (n = 27) and a lack of activity in the G6PDH counterscreen, IC₅₀ > 25 μM (n = 27). The chemotype was aggressively modified in the

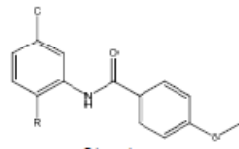


shaded regions of the diagram as part of our SAR strategy. A total of 102 compounds have been tested to date that relate to this scaffold. Of these, 83 were synthesized and 19 were purchased. All compounds, regardless of source, were purified and analyzed by LCMS and NMR for structural integrity and purity prior to assessment in assays.

A. Carboxylic acid isosteres

In most cases, replacement of the carboxylic acid with traditional isosteres resulted in loss of TbHK1 potency. Primary amides, sulfonamides, esters, or the use of an oxadiazolone were incorporated to mimic the hydrogen bonding and acidic nature of the carboxylic acid; however, all of these were found to be inferior to the parent. Installation of a nitro group, nitrile, a hydroxyl group or hydrogen at that position also resulted in no observable potency on TbHK1. Comparable activity to the carboxylic acid was achieved on substitution with a tetrazole, resulting in a TbHK1 IC₅₀ = 10.4 μM (SID 99344412/CID 16124577). All compounds in this set did not interfere in the G6PDH counterscreen and possessed EC₅₀s in the IMR90 cytotoxicity assay of > 25 μM (Table 2).

Table 2. SAR summary for compounds with carboxylic acid isosteric replacements

Entry	PubChem ID	Internal Center Number	*	 Structure	Potency mean (μM) (n = # replicates)				Selectivity G6PDH :TbHK1	IMR90 EC ₅₀ μM	% HgIk inhibition at 10 μM	% BSF growth inhibition at 10 μM
					TbHK1		G6PDH					
					n	IC ₅₀ μM	n	IC ₅₀ μM				
				R								
1	CID 1254149 SID 93575727	KUC106623N	S	CO ₂ H	27	9.1	27	> 25	> 2.7	> 25	7.8 ± 21.8	38 ± 5.7
2	CID 44443674 SID 96022036	KUC105792N	S	CO ₂ Me	3	> 25	3	> 25	NA	> 25	18.2 ± 5.5	0
3	CID 46391919 SID 99344413	KUC106630N	S	CONH ₂	3	> 25	3	> 25	NA	> 25	17.9 ± 7.5	35 ± 2
4	CID 46173039 SID 96022035	KUC105791N	S	SO ₂ NH ₂	3	> 25	3	> 25	NA	> 25	11.1 ± 8.5	37 ± 7
5	CID 16124577 SID 99344412	KUC105991N- 07	S	tetrazole	6	10.4	6	> 25	> 2.4	> 25	NA	33 ± 2
6	CID 46391918 SID 99344411	KUC106629N	S	oxadiazolone	3	> 25	3	> 25	NA	> 25	30.1 ± 6.9	0
7	CID 46173040 SID 96022037	KUC105793N	S	NO ₂	3	> 25	3	> 25	NA	> 25	0	38 ± 13
8	CID 46173041 SID 96022038	KUC105794N	S	CN	3	> 25	3	> 25	NA	> 25	0	0
9	CID 346039 SID 93618293	KUC105711N	P	H	3	> 25	3	> 25	NA	> 25	0	7.9 ± 0.9
10	CID 16099768 SID 99380772	KUC107302N	S	OH	3	> 25	3	> 25	NA	> 25	22.2 ± 0.67	36 ± 3

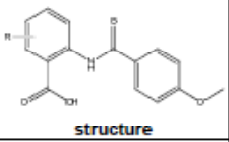
*S = synthesized; P = Purchased

B. Benzoic Acid Substitution

The 4-chlorophenyl substituent was targeted as a means of modulating the pKa of the benzoic acid and assessing the effect of different groups on the ring. Exchange of the 4-chloro group with 4-bromine was beneficial, resulting in a slight improvement in TbHK1 potency as compared to the parent (entry 2, SID 97302149 /CID 46245547, IC₅₀ = 6.9 μM); however other halides (entries 3-4), electron withdrawing or donating substituents (entries 5-6), larger substituents such as phenyl (entry 8), simple methyl substitution at the 4-position (entry 9), including removal of the 4-chloro group altogether (entry 10), resulted in erosion or complete loss of TbHK1 potency (Table 3). Moving the 4-chloro group to the 5-position was also not tolerated (entry 7). The effect of introducing other substituents on this ring while retaining the 4-chloro group was also surveyed. The introduction of a bromine at the 5-position notably improved potency (entry 12, IC₅₀ = 4.6 μM) as compared to the parent (entry 1) while the installation of a 5-methyl group (entry 13) resulted in a marginal loss in potency. Interestingly, the 5 position appears to tolerate some substitution in concert with the 4-chloro group and may represent an opportunity to further refine the potency profile of this scaffold. Compounds with substitutions at either the 3- and 6-positions with the 4-chloro group retained are being prepared, as the 4-substituent has been determined to be critical to maintaining reasonable TbHK1 potency, possibly as a function of both size and electronics, and at present, some advantage has been made by functionalizing

alternative positions (C3, C5 or C6). All completed compounds in this set did not interfere in the G6PDH counterscreen and possessed EC₅₀s in the IMR90 cytotoxicity assay of > 25 μM.

Table 3. SAR summary for substitution on the benzoic acid moiety

Entry	PubChem ID	Internal Center Number	*	 structure	Potency mean (μM) (n = # replicates)				Selectivity G6PDH: TbHK1	IMR90 EC ₅₀ μM	% hGik inhibition at 10 μM	% BSF growth inhibition at 10 μM
					TbHK1		G6PDH					
					n	IC ₅₀ μM	n	IC ₅₀ μM				
1	CID 1254149 SID 93575727	KUC105623N	S	4-Cl	27	9.1	27	> 25	> 2.7	> 25	7.8 ± 2.1.8	38 ± 5.7
2	CID 46245547 SID 97302149	KUC105928N	S	4-Br	3	6.9	3	> 25	> 3.6	> 25	0	43.8 ± 11
3	CID 46846332 SID 99234251	KUC106463N	S	4-I	3	14.2	3	> 25	> 1.8	> 25	0	28 ± 7
4	CID 16785950 SID 96022045	KUC105801N	P	4-F	3	24.8	3	> 25	~ 1	> 25	0	55 ± 17
5	CID 46245543 SID 97302143	KUC105921N	S	4-CF ₃	3	17.0	3	> 25	> 1.5	> 25	10.5 ± 10.7	33 ± 2.7
6	CID 178557 SID 93575728	KUC105624N	S	4-OMe	3	> 25	3	> 25	NA	> 25	6.9 ± 6.8	16 ± 8
7	CID 16776181 SID 93618295	KUC105713N	S	5-Cl	3	> 25	3	> 25	NA	> 25	0	21 ± 11
8	CID 46245545 SID 97302145	KUC105923N	S	4-Ph	3	> 25	3	> 25	NA	> 25	0	37.7 ± 4.4
9	CID 46839339 SID 99222886	KUC105995N	S	4-Me	3	> 25	3	> 25	NA	> 25	0	39 ± 2
10	CID 721421 SID 99234246	KUC106458N	P	4-H	3	> 25	3	> 25	NA	> 25	0	43 ± 11
11	CID 46931015 SID 99437304	KUC107589N	S	3,4-di-Cl	3	> 25	3	> 25	NA	> 25	10.6 ± 7.8	12 ± 7
12	CID 46916185 SID 99380766	KUC107296N	S	4-Cl, 5-Br	3	4.6	3	> 25	> 5.4	> 25	22.3 ± 6.4	43 ± 12
13	CID 46916184 SID 99380765	KUC107295N	S	4-Cl, 5-Me	3	10.3	3	> 25	> 2.4	> 25	17.6 ± 3.9	30 ± 10

*S = Synthesized; P = Purchased

C. Amide Linker Modifications

The amide linker portion of the scaffold was particularly sensitive to modification. Any attempt to methylate the nitrogen (entry 2, Table 4), migrate the amide and associated appendage to the 3-position of the benzoic acid moiety (entry 5), truncate or elongate the linker region (entries 3, 6-7), or replace the amide with a sulfonamide resulted in complete loss of TbHK1 potency.

Table 4. SAR summary for substitution of the amide linker region

Entry	CID	Internal Center Number	*	Structure		Potency mean (μM) (n = # replicates)				Selectivity G6PDH: TbHK1	IMR90 EC ₅₀ μM	% hGik inhibition at 10 μM	% BSF growth inhibition at 10 μM
				X	R	TbHK1		G6PDH					
						n	IC ₅₀ μM	n	IC ₅₀ μM				
1	CID 1254149 SID 93575727	KUC105823N	S	2-NHCO	4-OMe	27	9.1	27	> 25	> 27	> 25	7.8 ± 21.8	38.0 ± 5.7
2	CID 46245544 SID 97302144	KUC105922N	S	2-NMeCO	4-OMe	3	> 25	3	> 25	NA	> 25	6.7 ± 7.3	0
3	CID 66674 SID 97302136	KUC105914N	S	2-NH	4-OMe	3	> 25	3	> 25	NA	> 25	0	34.4 ± 5.4
4	CID 45464172 SID 97302134	KUC105912N	S	2-NHSO ₂	4-OMe	3	> 25	3	> 25	NA	> 25	0	26.6 ± 2.5
5	CID 25732782 SID 97302150	KUC105929N	S	3-NHCO	4-OMe	3	> 25	3	> 25	NA	> 25	0	0
6	CID 839406 SID 99222684	KUC105993N	S	2-NHCOCH ₂	4-OMe	3	> 25	3	> 25	NA	> 25	0	14.0 ± 5
7	CID 45436184 SID 99222685	KUC105994N	S	2-NHCOCH ₂	3-OMe	3	> 25	3	> 25	NA	> 25	0	9.0 ± 6

*S = Synthesized; P = Purchased

Other analogs in this set that were pursued included compounds that featured a fused amide moiety (Figure 15). Fusion of the amide either to the methoxyphenyl appendage or the benzoic acid region was not tolerated.

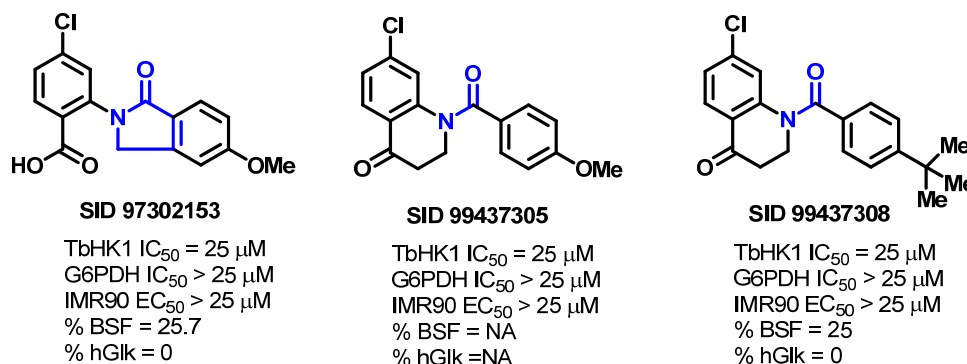


Figure 15. Fused amide analogs and associated data

This data suggests, in concert with the data collected for carboxylic acid isosteric replacements in Table 2 and 3-substitution on the benzoic acid moiety (see Table 3, entry 11), that interference with hydrogen bonding (possibly between the acid functionality and the amide N-H) is detrimental.

D. Amidoaryl Modifications

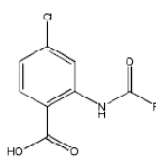
The parental 4-methoxyphenyl moiety (parent: SID 24798131/CID 1254149) was probed extensively through structural variation to determine if any potency could be gained on TbHK1 as compared to the hit compound (Table 5). Migration of the 4-methoxy group to either the 3- or 2-positions on the ring resulted in progressively worse potencies, respectively. Comparable potency to that of the parent was obtained with a benzodioxole group (entry 7, TbHK1 IC_{50} = 9.4 μ M); however, the similarly substituted 3,4-dimethoxyphenyl derivative (entry 6) demonstrated nearly a 2-fold loss in potency.

A series of analogues were also prepared that replaced the 4-methoxyphenyl group with various heterocycles or non-aromatic, cyclic entities that positioned polar functionality in the region where the 4-methoxy substituent of the parent resides (entries 9-17). In all cases, complete loss of TbHK1 activity was observed. Analogously, replacement of the complete methoxyphenyl moiety with linear aliphatic units was not tolerated (entries 19-23). Simple alterations (4-methoxy group \rightarrow 4-Cl, 4- CF_3 , or 4-H) were also inferior.

Guided by the fact that polar functionality occupying similar space to the 4-methoxy substituent was undesirable, the team pursued analogues bearing lipophilic groups in that region of space. The 4-ethylphenyl derivative was the first of these that produced a 3-fold boost in potency (SID 25734182/ CID 97302135, entry 34, TbHK1 IC_{50} = 3.0 μ M). This region of space was further characterized with several analogues bearing branched or cyclic alkyl groups at the 3- or 4-positions (entries 32-42).

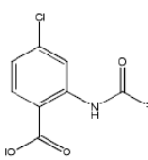
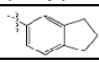
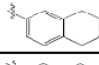
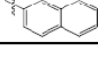
Migration of branched groups to the 3-position of the ring, again, resulted in loss of observable TbHK1 activity ($> 25 \mu$ M); however, a few analogues were identified with improved TbHK1 activity when the 4-substituent was modified, specifically SID 99222689/ CID 883362 (R = 4-*t*-butylphenyl, IC_{50} = 2.1 μ M) and SID 99344415/ CID 46891921 (R = 4-*t*-pentylphenyl, IC_{50} = 2.4 μ M). Clearly, the data suggests that small, branched, lipophilic groups off of C4 are advantageous. That binding region also appears to concurrently accommodate some small lipophilic group off of C3, as evidenced by a few ring-fused analogs that occupy C3 and C4 simultaneously (entries 43-45). For these compounds, there was some modest compromise in TbHK1 activity, but these changes were still well-tolerated (IC_{50} range = 4.8 – 5.4 μ M). A handful of analogs further exploring this region of space are currently in development to see if any enhancement of potency can be achieved. All compounds surveyed to date did not interfere in the G6PDH counterscreen and possessed EC_{50} s in the IMR90 cytotoxicity assay of $> 25 \mu$ M.

Table 5. SAR summary for modification of the amidoaryl component

Entry	PubChem ID	Internal Center Number	 Structure	Potency mean (μM) (n = # replicates)				Selectivity G6PDH: TbHK1	IMR90 EC ₅₀ μM	% hGik inhibition at 10 μM	% BSF growth inhibition at 10 μM
				TbHK1		G6PDH					
				n	IC ₅₀ μM	n	IC ₅₀ μM				
1	CID 1254149 SID 93575727	KUC 105623N	4-Ome-phenyl	27	9.1	27	> 25	> 2.7	> 25	7.8 \pm 21.8	38.0 \pm 5.7
2	CID 2233523 SID 93618294	KUC 105712N	3-Ome-phenyl	3	17.9	3	> 25	> 1.4	> 25	0	0
3	CID 16777607 SID 96022042	KUC 105798N	2-Ome-phenyl	3	25	3	> 25	NA	> 25	0	10.0 \pm 7
4	CID 45436333 SID 99222683	KUC 105992N	4-OCF ₃ -phenyl	3	25	3	> 25	NA	> 25	13.1 \pm 9.7	40.0 \pm 3
5	CID 763465 SID 93618301	KUC 105719N	4-OEt-phenyl	3	20.7	3	> 25	> 1.2	> 25	9.4 \pm 12.0	0
6	CID 1121964 SID 93618302	KUC 105720N	3,4-di-Ome-phenyl	3	15.5	3	> 25	> 1.6	> 25	20.1 \pm 21.1	23.0 \pm 6
7	CID 16777892 SID 99222695	KUC 106004N	benzodioxole	3	9.4	3	> 25	> 2.7	> 25	0	20.0 \pm 15
8	CID 16772990 SID 99222696	KUC 106005N	3,4,5-tri-Ome-phenyl	3	25	3	> 25	NA	> 25	0	31.0 \pm 4
9	CID 16770417 SID 97302142	KUC 105920N	3-furan	3	25	3	> 25	NA	> 25	0	0
10	CID 46245555 SID 97302155	KUC 105934N	oxazole	3	25	3	> 25	NA	> 25	0	21.2 \pm 8.5
11	CID 46846337 SID 99234262	KUC 106464N	2-thiophene	3	25	3	> 25	NA	> 25	30.3 \pm 13.4	38.0 \pm 5
12	CID 13849638 SID 97302148	KUC 105926N	3-thiophene	3	25	3	> 25	NA	> 25	0	0
13	CID 16771553 SID 97302151	KUC 105930N	4-pyridine	3	25	3	> 25	NA	> 25	0	19.3 \pm 6.3
14	CID 43354303 SID 99234245	KUC 106457N	4-MeO-3-pyridyl	3	25	3	> 25	NA	> 25	0	42.0 \pm 10
15	CID 46245549 SID 97302154	KUC 105933N	N-morpholine	3	25	3	> 25	NA	> 25	0	0
16	CID 46846330 SID 99234248	KUC 106460N	N-4-pyridone	3	25	3	> 25	NA	> 25	0	8.0 \pm 1
17	CID 28777638 SID 99234250	KUC 106462N	4-pyran	3	25	3	> 25	NA	> 25	0	3.0 \pm 2
18	CID 46846331 SID 99234249	KUC 106461N	3-benzofuran	3	25	3	> 25	NA	> 25	0	NA
19	CID 239963 SID 97302152	KUC 105931N	methyl	3	25	3	> 25	NA	> 25	0	0
20	CID 25767407 SID 99234243	KUC 106455N	n-pentyl	3	25	3	> 25	NA	> 25	0	20.0 \pm 7
21	CID 43170501 SID 99234244	KUC 106456N	n-hexyl	3	25	3	> 25	NA	> 25	0	23.0 \pm 8
22	CID 43125186 SID 99222693	KUC 106002N	n-heptane	3	25	3	> 25	NA	> 25	0	16.0 \pm 10
23	CID 16776792 SID 99222694	KUC 106003N	phenyl	3	25	3	> 25	NA	> 25	0	28.0 \pm 4
24	CID 587114 SID 96022041	KUC 105797N	4-Cl-phenyl	3	25	3	> 25	NA	> 25	0	28.0 \pm 19
25	CID 25734160 SID 99344416	KUC 106833N	4-I-phenyl	3	16.3	3	> 25	> 1.5	NA	22.9 \pm 6.6	33.0 \pm 6
26	CID 45436122 SID 99234263	KUC 106465N	4-CF ₃ -phenyl	3	25	3	> 25	NA	> 25	0	28.0 \pm 3

*S Synthesized; P = Purchased

Table 5. Continued - SAR summary for modification of the amidoaryl component

Entry	PubChem ID	Internal Center Number	 Structure	Potency mean (μM) (n = # replicates)				Selectivity G6PDH: TbHK1	IMR90 EC ₅₀ μM	% hGIK inhibition at 10 μM	% BSF growth inhibition at 10 μM
				TbHK1		G6PDH					
				n	IC ₅₀ μM	n	IC ₅₀ μM				
27	CID 46856249 SID 99245524	KUC106493N	4-phenyl-phenyl	3	22.3	3	> 25	> 1.1	> 25	27.6 \pm 7.2	NA
28	CID 46856248 SID 99245521	KUC106490N	4-benzyl-phenyl	3	13.7	3	> 25	> 1.8	> 25	0	5.03 \pm 4.0
29	CID 7128189 SID 99234241	KUC106453N	3-methyl-phenyl	3	22.3	3	> 25	> 1.1	> 25	0	24.0 \pm 12
30	CID 839504 SID 99245526	KUC106495N	3,4-di-methyl-Ph	3	10.7	3	> 25	> 2.3	> 25	0	NA
31	CID 16772479 SID 99245525	KUC106494N	2,4-di-methyl-Ph	3	25	3	> 25	NA	> 25	12.5 \pm 5.5	36.0 \pm 13
32	CID 46846329 SID 99234247	KUC106459N	3- <i>i</i> -propyl-phenyl	3	25	3	> 25	NA	> 25	0	NA
33	CID 16777984 SID 99222892	KUC106001N	4-methyl-phenyl	3	13.8	3	> 25	> 1.8	> 25	0	30.0 \pm 3
34	CID 25734182 SID 97302135	KUC105913N	4-ethyl-phenyl	3	3.0	3	> 25	> 8.3	> 25	0	26.6 \pm 11
35	CID 46846328 SID 99234242	KUC106454N	4- <i>n</i> -propyl-phenyl	3	4.5	3	> 25	> 5.6	> 25	16.8 \pm 3.9	37.0 \pm 7
36	CID 45436131 SID 99222890	KUC105999N	4- <i>i</i> -propyl-phenyl	3	2.9	3	> 25	> 8.6	> 25	0	34.0 \pm 10
37	CID 883382 SID 99222889	KUC105998N	4- <i>t</i> -butyl-phenyl	3	2.1	3	> 25	> 11.9	> 25	0	4.0 \pm 8
38	CID 46846338 SID 99234264	KUC106466N	4-isobutyl-phenyl	3	7.3	3	> 25	> 3.4	> 25	19.5 \pm 8.4	17.0 \pm 5
39	CID 46891921 SID 99344415	KUC106832N	4- <i>t</i> -pentyl-phenyl	3	2.4	3	> 25	> 10.4	> 25	26.0 \pm 8.3	11.0 \pm 4
40	CID 46856250 SID 99245527	KUC106496N	4-cyclopropylphenyl	6	5.8	6	> 25	> 4.3	> 25	NA	NA
41	CID 46931013 SID 99437302	KUC107587N	4-(1-methylcyclopropylphenyl)	3	4.9	3	> 25	> 5.1	> 25	NA	NA
42	CID 46891922 SID 99344417	KUC106834N	4-cyclobutylphenyl	6	7.2	6	> 25	> 3.5	> 25	35.4 \pm 8.0	21.0 \pm 6
43	CID 46891920 SID 99344414	KUC106831N	4-cyclopentylphenyl	3	7.9	3	> 25	> 3.2	> 25	21.1 \pm 8.4	31.0 \pm 10
44	CID 45436219 SID 99245523	KUC106492N		3	4.8	3	> 25	> 5.2	> 25	12.2 \pm 4.0	NA
45	CID 45436278 SID 99344409	KUC106828N		3	4.9	3	> 25	> 5.1	> 25	NA	NA
46	CID 9321758 SID 99245522	KUC106491N		3	5.4	3	> 25	> 4.6	> 25	11.5 \pm 6.3	NA

*S Synthesized, P = Purchased

E. Tandem Modifications

Those structural features found to improve TbHK1 activity were combined in anticipation of a synergistic effect (Table 6). For instance, exchange of the chlorine of the parent (entry 1) for a bromine was determined to be acceptable, as was the optimization of the amidoaryl moiety with branched alkyl groups off of the 4-position. In the course of our investigation, the bromine and 4-

ethylphenyl or 4-*tert*-butylphenyl combination were studied (entries 2 and 3), affording an improved TbHK1 activity of $IC_{50} = 5.5 \mu\text{M}$ and $2.4 \mu\text{M}$, respectively. As it has been shown, the best amidoaryl 4-substituent is a *t*-butyl group. This alteration was coupled with other features such as the tetrazole (entry 4), which was tolerated in place of the carboxylic acid. Additionally, the substitution pattern of the benzoic acid moiety of $R_1 = \text{Cl}$, $R_2 = \text{Br}$ (entry 7) was discovered to be the most beneficial optimization, resulting in a submicromolar inhibition of TbHK1 and culminating in the declaration of a probe compound for this project.

Table 6. Survey of combined effects of optimized functionality

Entry	PubChem ID	Internal Center Number	*	Structure				Potency mean (μM) (n = # replicates)				Selectivity G6PDH: TbHK1	IMR90 EC_{50} μM	% hGik inhibition at $10 \mu\text{M}$	% BSF growth inhibition at $10 \mu\text{M}$
				R1	R2	R3	R4	TbHK1		G6PDH					
								n	$IC_{50} \mu\text{M}$	n	$IC_{50} \mu\text{M}$				
1	CID 1254149 SID 93575727	KUC105623N	S	Cl	H	CO_2H	OMe	27	9.1	27	> 25	> 2.7	> 25	7.8 ± 21.8	38.0 ± 5.7
2	CID 46839341 SID 99222391	KUC106000N	S	Br	H	CO_2H	ethyl	3	5.5	3	> 25	> 4.5	> 25	0	19.0 ± 1
3	CID 46916166 SID 99380767	KUC107297N	S	Br	H	CO_2H	<i>t</i> -butyl	3	2.4	3	> 25	> 10.4	> 25	26.2 ± 4.8	13.0 ± 6
4	CID 46916168 SID 99380773	KUC107303N	S	Cl	H	tetrazole	<i>t</i> -butyl	3	3.5	3	> 25	> 7.1	> 25	28.4 ± 5.3	29.0 ± 6
5	CID 40910104 SID 99380765	KUC107295N	S	Cl	Me	CO_2H	OMe	3	10.3	3	> 25	> 2.4	> 25	17.6 ± 3.9	30.0 ± 10
6	CID 46916165 SID 99380766	KUC107296N	S	Cl	Br	CO_2H	OMe	3	4.6	3	> 25	> 5.4	> 25	22.3 ± 6.4	43.0 ± 12
7	CID 46931017 SID 99437306	KUC107591N	S	Cl	Br	CO_2H	<i>t</i> -butyl	6	0.98	6	> 25	> 25.5	> 25	**NA	6.9 ± 3.0
8	CID 46947875 SID 99460393	KUC107686N	S	Cl	Cl	CO_2H	<i>t</i> -butyl	3	1.4	3	> 25	> 17.9	> 25	0	35.0 ± 11
9	CID 40766810 SID 103023816	KUC107739N	S	Cl	F	CO_2H	<i>t</i> -butyl	3	2.8	3	> 25	> 8.9	> 25	0	32.0 ± 11

*S = Synthesized; P = Purchased

**% hGik inhibition was not calculated, but an IC_{50} was obtained = $46.3 \pm 6.9 \mu\text{M}$

3.5 Cellular Activity

Compounds were evaluated in a human IMR90 growth inhibition assay (AID 449725) to assess mammalian cytotoxicity. All compounds in the series possessed EC_{50} s in the IMR90 cytotoxicity assay of $> 25 \mu\text{M}$. Data from the whole parasite BSF assay, while not required for probe criteria, was collected for many of the compounds in this series. Most compounds were assessed at a single concentration of $10 \mu\text{M}$ for percent growth inhibition of parasites and all registered in the range of 0-55%. The SAR profile relating to the percent BSF inhibition is not quite clear at this point in time; however, the compounds do show toxicity towards parasites to varying degrees. Select examples are shown in Figure 16 and in the preceding SAR tables.

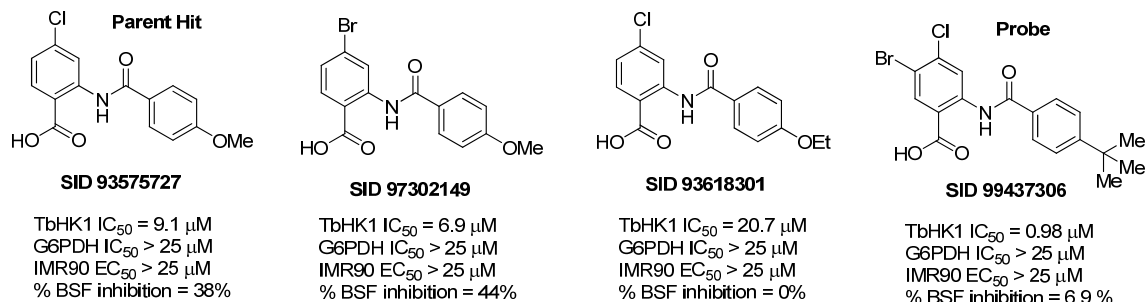


Figure 16. Select examples of cellular IMR90 and percent BSF inhibition data

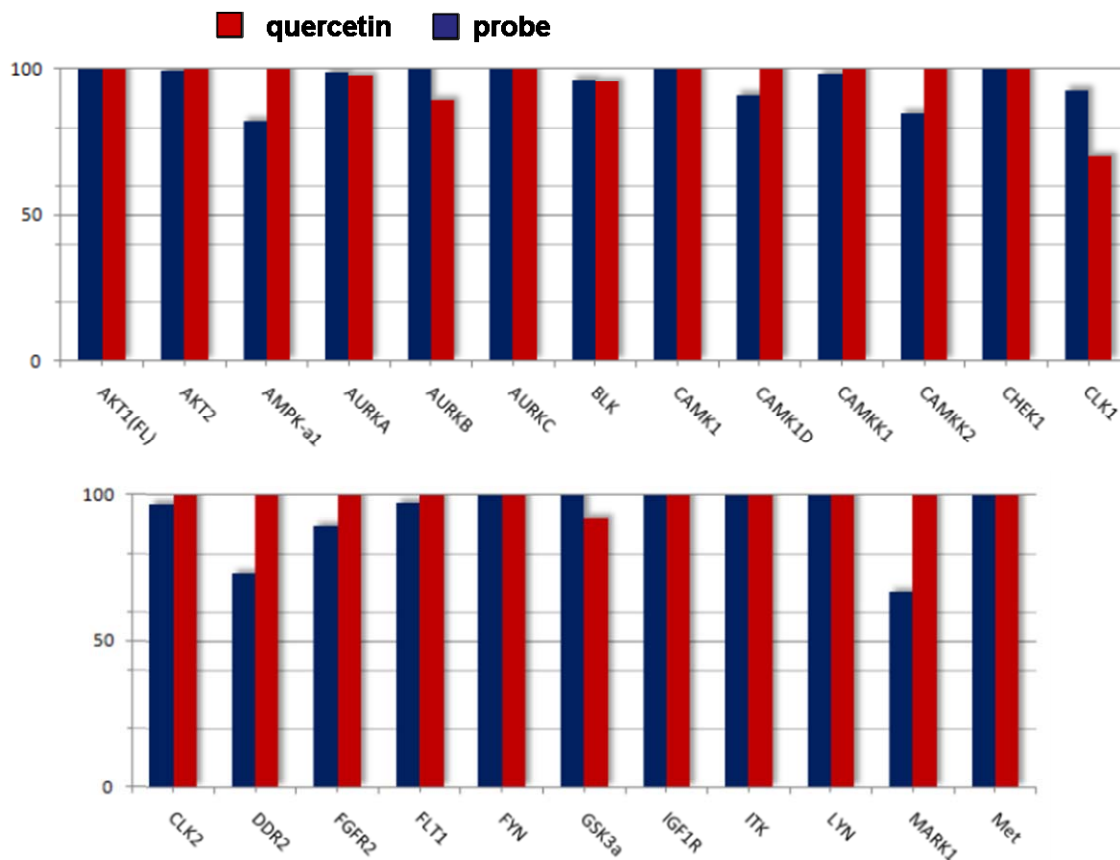
3.6 Profiling Assays

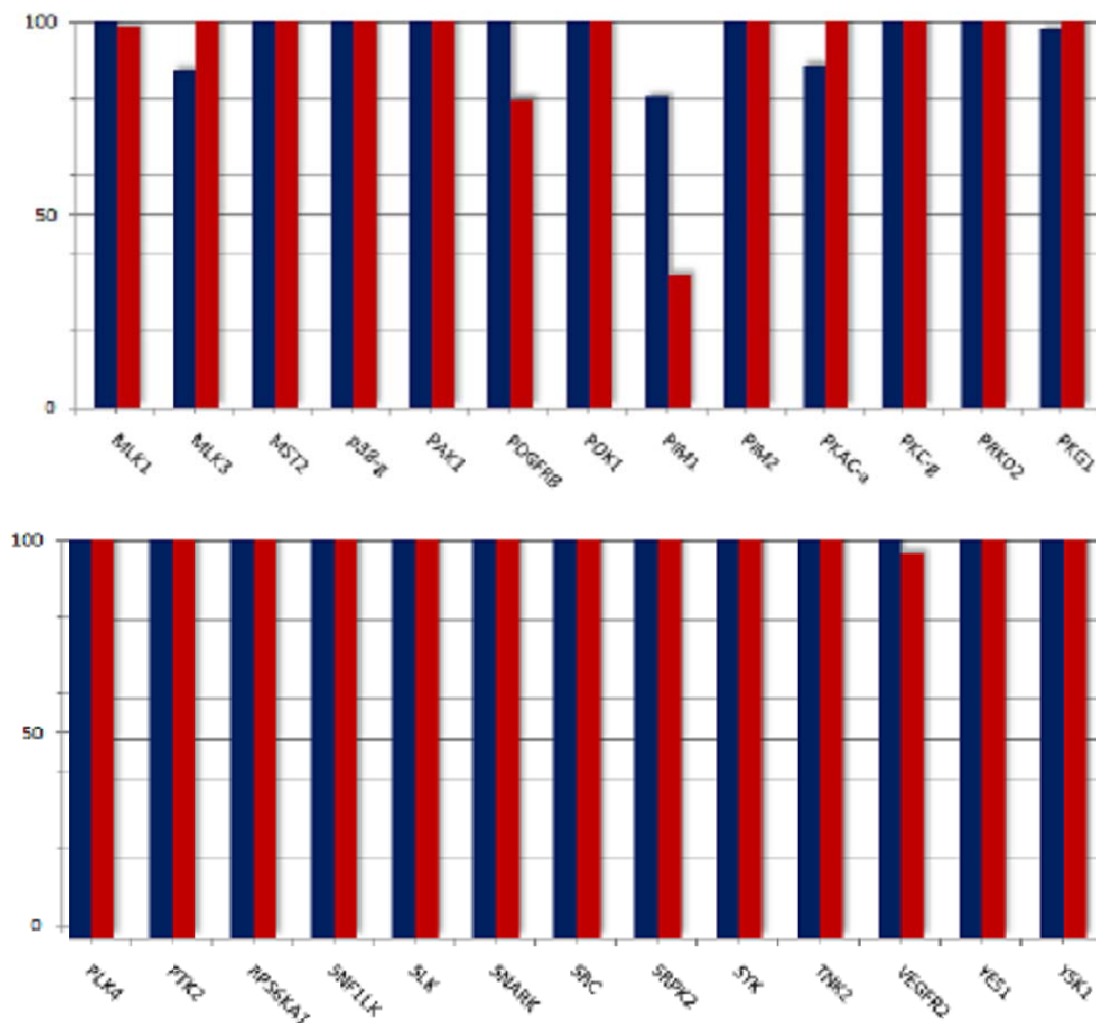
The probe compound ML205, SID 99437306, CID 46931017 and the purified prior art compound quercetin (SID 99460891/ CID 5280343) were profiled at 5 μM in a 50-member kinase panel to assess differences in selectivity between the two compounds [16].

Kinase	Family	PROBE	QUERCETIN
		% Activity Remaining SID 99437306	% Activity Remaining SID 99460891
AKT1(FL)	AGC	100	100
AKT2	AGC	99.4	100
AMPK- α 1	CAMK	82.2	100
AURKA	Other	98.8	97.9
AURKB	Other	100	89.4
AURKC	Other	100	100
BLK	TK	96.5	95.7
CAMK1	CAMK	100	100
CAMK1D	CAMK	91.3	100
CAMKK1	Other	98.4	100
CAMKK2	Other	84.8	100
CHEK1	CAMK	100	100
CLK1	CMGC	92.8	70.3
CLK2	CMGC	96.8	100
DDR2	TK	73.1	100
FGFR2	TK	89.4	100
FLT1	TK	97.4	100
FYN	TK	100	100
GSK3 α	CMGC	100	92.1
IGF1R	TK	100	100
ITK	TK	100	100
LYN	TK	100	100
MARK1	CAMK	66.9	100
Met	TK	100	100
MLK1	TKL	100	98.6

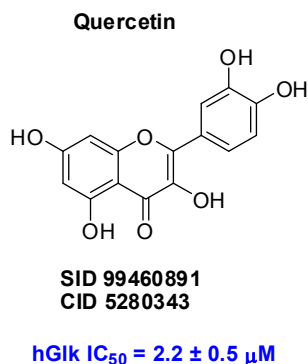
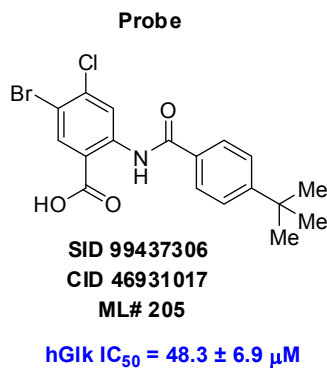
Kinase	Family	PROBE	QUERCETIN
		% Activity Remaining SID 99437306	% Activity Remaining SID 99460891
MLK3	TKL	87.4	100
MST2	STE	100	100
p38- α	CMGC	100	100
PAK1	STE	100	100
PDGFRB	TK	100	80
PDK1	AGC	100	100
PIM1	CAMK	80.5	34.3
PIM2	CAMK	100	100
PKAC- α	AGC	88.8	100
PKC- α	AGC	100	100
PRKD2	CAMK	100	100
PKG1	AGC	98	100
PLK4	Other	100	100
PTK2	TK	100	100
RPS6KA1	AGC	100	100
SNF1LK	CAMK	100	100
SLK	STE	100	100
SNARK	CAMK	100	100
SRC	TK	100	100
SRPK2	CMGC	100	100
SYK	TK	100	100
TNK2	TK	100	100
VEGFR2	TK	100	96.8
YES1	TK	100	100
YSK1	STE	100	100

For most of the kinases assayed, both the probe and quercetin showed relatively low (0-10%) inhibition. In the case of PIM1, quercetin showed significant inhibition (~66%) while the probe compound demonstrated inhibition at ~ 20%. Profiling data for all kinases was plotted as percent activity remaining vs. kinases profiled, represented below:





Human glucokinase was not available as part of the panel, but the Assay Provider assessed compounds for this target at 10 μ M (AID 492951). The probe compound did not significantly inhibit hGik (IC_{50} = 48.3 μ M) while quercetin inhibited the same target with an IC_{50} of 2.2 μ M.



4 Discussion

4.1 Comparison to existing art and how the new probe is an improvement

The HTS effort that identified a viable hit scaffold and the optimization of the parent hit SID 24798131/CID 1254149 with rTbHK1 $IC_{50} = 9.1 \mu\text{M}$ to a probe that inhibits rTbHK1 in the submicromolar range is a significant achievement given the limited leads and therapeutics available. This project has delivered a probe that meets all of the criteria set forth in the CPDP and significantly improves upon prior art in the (1) potency on the *in vitro* rTbHK1 target, (2) structural improvements to avoid reactive functionality, and (3) better selectivity against hGik (a related human kinase) and PIM1 (important in cell cycle regulation and apoptosis). Given that quercetin has been shown to inhibit a variety of targets, thus limiting its use with respect to definitive hexokinase pathway investigation, the increased value of the probe defined here is in its ability to avoid these off-target liabilities [8].

Table 7. Comparison of quercetin and probe

Parameter or Biological Characteristics	Desired Probe Characteristic	Quercetin	Probe ML205	Probe meets criteria?
SID	NA	99460891	99437306	NA
CID	NA	5280343	46931017	NA
rTbHK1 potency (IC_{50} , nM)	$IC_{50} \leq 1000$ nM	$IC_{50} = 22400$ nM	$IC_{50} = 976$ nM	Yes ✓
selectivity vs G6PDH reporter enzyme (nM)	$IC_{50} \geq 25000$ nM	$IC_{50} > 25000$ nM	$IC_{50} > 25000$ nM	Yes ✓
Biological Mode of Action/Assessment	<i>in vitro</i>	<i>in vitro</i>	<i>in vitro</i>	Yes ✓
Pharmacology/Mode of Action (allosteric/covalent, etc)	mixed inhibition with respect to ATP	mixed inhibition with respect to ATP	mixed inhibition with respect to ATP	Yes ✓
Cellular Toxicity in IMR90 cells	$EC_{50} > 25000$ nM (or 10x BSF LD_{50})	$EC_{50} > 25000$ nM	$EC_{50} > 25000$ nM	Yes ✓
Structural Features to Avoid	Non-flavinol	Flavinol	Non-flavinol	Yes ✓
selectivity vs human glucokinase (hGik) % inhibition at 10 μM or IC_{50}	$IC_{50} > 10x$ TbHK1 IC_{50}	$IC_{50} = 2200$ nM (nonselective)	$IC_{50} = 48300$ nM	Yes ✓
Cytotoxicity towards whole BSF parasites (% inhibition at 10 μM or LD_{50}) - not required	$LD_{50} < 25000$ nM	$LD_{50} = 2950$ nM	% inhibition at 10 μM = 6.9	Not required
off target liability - not required	selective against a panel of kinases	promiscuous against various kinases, specifically hGik and PIM1	selective against a panel of kinases	Not required

4.2 Mechanism of Action Studies

In an attempt to better understand the nature of the inhibition associated with these compounds on TbHK1, an additional study was completed by the assay provider, Dr. James Morris (Fig. 17). Preliminary studies suggest that SID 99437306/ CID 46931017 is a mixed inhibitor of TbHK1 with respect to ATP with a K_i of 0.695 μM . This is notable because screens for inhibitors of kinases have tended to yield competitive inhibitors that are frequently ATP analogues – SID 99437306/ CID 46931017 may represent a novel, non-ATP binding site scaffold for probe improvement against TbHK1.

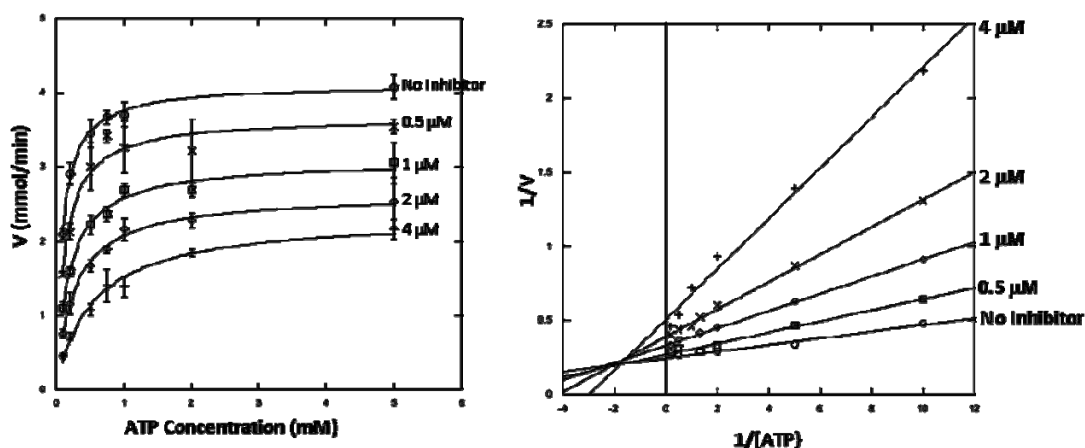


Figure 17. Michaelis-Menten and Lineweaver-Burk plots showing mixed inhibition of TbHK1 with respect to ATP using ML205, SID 99437306, CID 46931017.

4.3 Planned Future Studies

A probe advancement proposal was submitted to the NIH as of October 13, 2010, and has been subsequently approved. While some regions of the scaffold represented by probe ML205 were not amenable to SAR modification without adversely affecting potency, optimization was possible in four sectors that were investigated. There remain a few diversification points which were not included in this effort which may lead to improved profile and opportunity to refine physiochemical parameters. The following specific SAR plans are being implemented to address potency and cellular permeability.

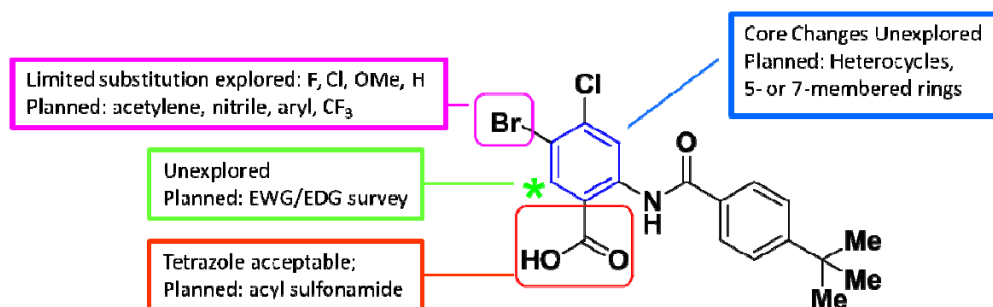


Figure 18. Planned SAR optimization for extended probe characterization

The areas highlighted above will be investigated to meet the goals of the project. Unaddressed areas of the structure are not being modified as these were extensively studied in the probe project leading to the development of ML205; however, these regions may be altered in the event that structural variation elsewhere gains sufficient activity. In the probe enhancement phase, the probe will be compared to quercetin and assessed in the following ways:

Parameter or Biological Characteristics	Quercetin	Probe ML205	Desired Optimized Probe
SID	99460891	99437306	NA
CID	5280343	46931017	NA
rTbHK1 potency (IC ₅₀ , nM)	IC ₅₀ = 22400 nM	IC ₅₀ = 976 nM	IC ₅₀ ≤ 500 nM
rTbHK1 potency (IC ₅₀ , nM) in ATP-regeneration coupled assay	unknown	unknown	IC ₅₀ ≤ 500 nM
Inhibit TbHK1 activity from <i>T. brucei</i> parasite lysate	IC ₅₀ = 24000 nM**	unknown	IC ₅₀ ≤ 500 nM
Cytotoxicity towards whole BSF parasites (% inhibition at 10 μM or LD ₅₀)	LD ₅₀ = 2950 nM	% inhibition at 10 μM = 6.9	LD ₅₀ of ≤ 1000 nM
Confirmation of action on the <i>in vivo</i> target, as determined by measuring the impact of compound on parasitic cellular G6P levels	unknown	unknown	> 30%
Selectivity vs yeast hexokinase	unknown	unknown	≤ 25% inhibition or IC ₅₀ > 10,000 nM
Selectivity vs human hexokinase 1	unknown	unknown	< 25% inhibition or IC ₅₀ > 10,000 nM
selectivity vs human glucokinase (hGlc) % inhibition at 10 μM or IC ₅₀	IC ₅₀ = 2200 nM (nonselective)	IC ₅₀ = 48300 nM	< 50% inhibition at 10 μM; IC ₅₀ > 10x TbHK1 IC ₅₀
selectivity vs G6PDH reporter enzyme (nM)	IC ₅₀ > 25000 nM	IC ₅₀ > 25000 nM	IC ₅₀ > 25000 nM
limited other off target liability (Luceome profiling)	promiscuous against various kinases, specifically hGlc and PIM1	selective against a panel of kinases	selective against a panel of kinases

*These values are provided as a guideline, but it should be noted that these can be highly variable and depend on pharmacokinetics as a whole. As a result, a compound may have acceptable PK due to the interplay of these characteristics while the individual characteristic may fall out of the desired guideline.

**TbHK activity (may be due to either TbHK1 or TbHK2)

Parameter or Biological Characteristics	Quercetin	Probe ML205	Desired Optimized Probe
<i>Demonstrate efficacy in the Leishmania promastigote assay</i>	unknown	unknown	informative, but not critical to probe status
Biological Mode of Action/Assessment	in vitro	in vitro	in vivo
Pharmacology/Mode of Action (allosteric/covalent, etc)	mixed inhibition with respect to ATP	mixed inhibition with respect to ATP	mixed inhibition with respect to ATP
Cellular Toxicity in IMR90 cells	EC ₅₀ > 25000 nM	EC ₅₀ > 25000 nM	EC ₅₀ > 25000 nM (or 10x BSF LD ₅₀)
Aqueous solubility 1x PBS buffer (ug/mL) pH 7.4	unknown	25.6 ug/mL	≥ 50 ug/mL
Aqueous stability (% remaining after 48 h)	unknown	100%	≥ 95%
cellular permeability (10 ⁻⁶ cm/s)	unknown	unknown	medium-high
microsomal stability t _{1/2} (mouse) [min]	unknown	unknown	20-40 min*
plasma protein binding	unknown	unknown	< 97%*
plasma stability	unknown	unknown	> 95%*
efficacy in acute infection mouse model	unknown	unknown	TBD mg/kg

*These values are provided as a guideline, but it should be noted that these can be highly variable and depend on pharmacokinetics as a whole. As a result, a compound may have acceptable PK due to the interplay of these characteristics while the individual characteristic may fall out of the desired guideline.

**TbHK activity (may be due to either TbHK1 or TbHK2)

Compounds will be provided by the KU SCC in sufficient quantities (500 mg – 1 gram) and purity for the proposed studies and will likely be further refined structurally to tune physiochemical and pharmacokinetic parameters necessary for adequate analysis in rodent models. Specifically, the probe will be assessed by the KU SCC and structurally optimized to:

- A. possess suitable aqueous solubility, stability, and cellular permeability
- B. possess reasonable microsomal stability, plasma protein binding and plasma stability
- C. be assessed for *in vivo* pharmacokinetics

5 References

1. WHO Media centre (2010). *Fact sheet N°259: African trypanosomiasis or sleeping sickness*. <http://www.who.int/mediacentre/factsheets/fs259/en/>.
2. Remme JH, Blas E, Chitsulo L, Desjeux PM, Engers HD, et al. (2002) Strategic emphases for tropical diseases research: a TDR perspective. *Trends Parasitol* 18:421–426.
3. Jacobs RT, Ding C. (2010) Recent advances in drug discovery for neglected tropical diseases caused by infective kinetoplastid parasites. *Annual Reports in Medicinal Chemistry* 45: 277-294.
4. Trinquier M, Perie J, Callens M, Opperdoes F, Willson M (1995) Specific inhibitors for the glycolytic enzymes of *Trypanosoma brucei*. *Bioorg. Med. Chem.* 3: 1423–1427.
5. Willson M, Sanejouand YH, Perie J, Hannaert V, Opperdoes F (2002) Sequencing, modeling, and selective inhibition of *Trypanosoma brucei* hexokinase. *Chem. Biol.* 9: 839–847.
6. Chambers JW, Fowler ML, Morris MT, Morris JC (2008) The antitrypanosomal agent lonidamine inhibits *Trypanosoma brucei* hexokinase 1. *Mol Biochem Parasitol* 158: 202–207.
7. Sharlow ER, Lyda, TA, Dodson, HC, Mustata G, Morris MT, Leimgruber SS, Lee K-H, Kashiwada Y, Close D, Lazo JS, Morris JC. (2010) A target-based high throughput screen yields *Trypanosoma brucei* hexokinase small molecule inhibitors with antiparasitic activity. *PLoS Negl Trop Dis.* 4: e659 (7 pages). PMID: PMC2854128
8. Dodson HC, Lyda TL, Chambers JW, Morris MT, Christensen KA, Morris JC (2010) Quercetin, a fluorescent bioflavonoid, inhibits *Trypanosoma brucei* hexokinase 1. *Experimental Parasitology*. *In press*.
9. Srivastava, A.K., (1985) Inhibition of phosphorylase kinase, and tyrosine protein kinase activities by quercetin. *Biochem. Biophys. Res. Commun.* 131: 1–5.
10. Matter, W.F., Brown, R.F., Vlahos, C.J., (1992) The inhibition of phosphatidylinositol 3-kinase by quercetin and analogs. *Biochem. Biophys. Res. Commun.* 186: 624– 631.
11. Boege, F., Straub, T., Kehr, A., Boesenberg, C., Christiansen, K., Andersen, A., Jakob, F., Kohrle, J. (1996) Selected novel flavones inhibit the DNA binding or the DNA religation step of eukaryotic topoisomerase I. *J. Biol. Chem.* 271: 2262–2270.
12. Solubility and stability data was outsourced to and collected by the Sanford-Burnham Center, Dr. Layton Smith.
13. Dreher SD, Dormer PG, Sandrock DL, Molander GA. (2008) Efficient cross-coupling of secondary alkyltrifluoroborates with aryl chlorides - reaction discovery using parallel microscale experimentation. *J. Am. Chem. Soc.* 130: 9257-9259.
14. Molander GA, Gormisky PE. (2008) Cross-coupling of cyclopropyl- and cyclobutyltrifluoroborates with aryl and heteroaryl chlorides. *J. Org. Chem.* 73: 7481-7485.
15. Koguro K; Oga T; Mitsui S; Orita R. (1998) Novel synthesis of 5-substituted tetrazoles from nitriles. *Synthesis* 6: 910-914.
16. Data obtained from Luceome Biotechnologies using the *KinaseSeeker™* assay. For information on the assay principle and method, please refer to: Jester, B. W.; Cox, K. J.; Gaj, A.; Shomin, C. D.; Porter, J. R.; Ghosh, I. "A Coiled Coil Enabled Split-Luciferase Three-Hybrid System: Applied Toward Profiling Inhibitors of Protein Kinases" *J. Am. Chem. Soc.* **2010**, *132*, 11727-11735. Assay design and method: Compounds were dissolved in DMSO and tested at a final concentration of 5 μ M in all experiments. Prior to initiating a profiling campaign, the compound was evaluated for false positive against split-luciferase. After it was determined that it did not inhibit the luciferase control at 5 μ M concentration, profiling was done in duplicate for against each kinase. The % Inhibition and % Activity Remaining was calculated using the following equation: % Inhibition = (ALUControl – ALUSample) /ALUControl x 100; % Activity Remaining = 100 - % Inhibition.